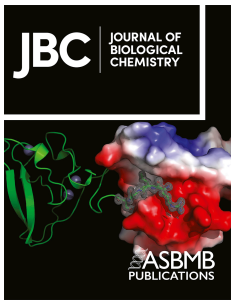

Regulation of Calcium entry by cyclic GMP signaling in *Toxoplasma gondii*

Miryam A. Hortua Triana, Karla M. Márquez-Nogueras, Mojtaba Sedigh Fazli, Shannon Quinn, Silvia N.J. Moreno

PII: S0021-9258(24)00147-9

DOI: https://doi.org/10.1016/j.jbc.2024.105771

Reference: JBC 105771

To appear in: *Journal of Biological Chemistry*

Received Date: 1 August 2023

Revised Date: 9 January 2024

Accepted Date: 28 January 2024

Please cite this article as: Hortua Triana MA, Márquez-Nogueras KM, Fazli MS, Quinn S, Moreno SNJ, Regulation of Calcium entry by cyclic GMP signaling in *Toxoplasma gondii*, *Journal of Biological Chemistry* (2024), doi: https://doi.org/10.1016/j.jbc.2024.105771.

Regulation of Calcium entry by cyclic GMP signaling in *Toxoplasma gondii*

Miryam A. Hortua Triana[1], Karla M. Márquez-Nogueras[1], Mojtaba Sedigh Fazli[2], Shannon Quinn[2] and Silvia N.J. Moreno[1,3]

[1]Center for Tropical and Emerging Global Diseases, [2]Department of Computer Science, and [3]Department of Cellular Biology, University of Georgia, Athens, Georgia 30602

Running title: Calcium and cGMP in *T. gondii*

[*]To whom correspondence should be addressed: Silvia N. J. Moreno, Department of Cellular Biology and Center for Tropical and Emerging Global Disease, 350A Paul D. Coverdell Center, University of Georgia, Athens, GA 30602. Tel.: 706-542-4736; Fax: 706-542-9493; E-mail: smoreno@uga.edu

Keywords: Calcium, signaling, cGMP, protein kinase G, invasion, egress, Toxoplasma gondii.

ABSTRACT

Ca^{2+} signaling impacts almost every aspect of cellular life. Ca^{2+} signals are generated through the opening of ion channels that permit the flow of Ca^{2+} down an electrochemical gradient. Cytosolic Ca^{2+} fluctuations can be generated through Ca^{2+} entry from the extracellular milieu or release from intracellular stores. In *Toxoplasma gondii*, Ca^{2+} ions play critical roles in several essential functions for the parasite like invasion of host cells, motility and egress. Plasma membrane Ca^{2+} entry in *T. gondii* was previously shown to be activated by cytosolic calcium and inhibited by the voltage-operated Ca^{2+} channel blocker nifedipine. However, Ca^{2+} entry in *T. gondii* did not show the classical characteristics of store regulation. In this work, we characterized the mechanism by which cytosolic Ca^{2+} regulates plasma membrane Ca^{2+} entry in extracellular *T. gondii* tachyzoites loaded with the Ca^{2+} indicator Fura 2. We compared the inhibition by nifedipine with the effect of the broad spectrum TRP channel inhibitor, anthranilic acid or ACA and we find that both inhibitors act on different Ca^{2+} entry activities. We demonstrate, using pharmacological and genetic tools, that an intracellular signaling pathway engaging cyclicGMP (cGMP), protein kinase G (PKG), Ca^{2+} and the phosphatidyl inositol phospholipase C (PI-PLC) affects Ca^{2+} entry and we present a model for crosstalk between cGMP and cytosolic Ca^{2+} for the activation of *T. gondii*'s lytic cycle traits.

INTRODUCTION

Toxoplasma gondii is an obligate intracellular parasite that infects approximately one third of the world's population (1). *T. gondii* causes disease by engaging in multiple rounds of a lytic cycle, which consists of invasion of host cells, replication inside a parasitophorous vacuole (PV), egress resulting in host cell lysis, and invasion of a new host cell (2, 3). Several key steps of the lytic cycle of *T. gondii* which are motility, attachment, invasion, and egress, are regulated by fluctuations in its cytosolic Ca^{2+} concentration ($[Ca^{2+}]_{cyt}$ (4, 5).

Ca^{2+} signaling plays important roles in the regulation of many cellular functions (6). However, the concentration of cytosolic Ca^{2+} ($[Ca^{2+}]_{cyt}$) is highly regulated, because sustained high cytosolic Ca^{2+} is toxic and may result in cell death. A variety of Ca^{2+} pumps, channels, and transporters, located at the plasma membrane (PM) and intracellular organelles (endoplasmic reticulum (ER), acidic stores, and mitochondria) are involved in regulating $[Ca^{2+}]_{cyt}$ (7).

In *T. gondii*, both Ca^{2+} entry and release from intracellular stores like the endoplasmic reticulum (ER) may initiate a cascade of signaling pathways that promote progression through the biological steps of the parasite's lytic cycle. Motile parasites loaded with fluorescent Ca^{2+} indicators or expressing genetically encoded calcium indicators (GECIs) showed Ca^{2+} oscillations (8, 9). Previous studies have shown that a rise in the $[Ca^{2+}]_{cyt}$ activates the motility machinery leading to egress. Blocking these cytosolic Ca^{2+} oscillations with BAPTA-AM (membrane permeable cytosolic Ca^{2+} chelator), blocks motility, conoid extrusion (apical tip of the parasite necessary for attachment), invasion, and egress from the host cell (4).

Extracellular Ca^{2+} entry was demonstrated to be key in these processes in both extracellular (10) and intracellular replicating tachyzoites (11). In previous work we showed that Ca^{2+} entry can be inhibited ~80% by voltage operated Ca^{2+} channel blockers like nifedipine (10) and ~50% by the wide-spectrum Transient Receptor Potential (TRP) channel inhibitor anthranilic acid (ACA) (12). Cytosolic Ca^{2+} itself enhanced Ca^{2+} entry by a mechanism that we termed Ca^{2+}-activated Ca^{2+}-entry and recent work from our lab demonstrated the participation of a TRP-like channel named TgTRPP2-L (12). However, the experimental evidence did not support that this calcium entry mechanism was regulated by store depletion as seen in mammalian cells by Store Operated Calcium Entry (SOCE) (13, 14). Furthermore, experiments testing surrogate ions like Mn^{2+} (10) and the

absence of the components of the SOCE pathway, STIM and ORAI, in the *T. gondii* genome supported this notion (15).

Several recent studies demonstrated that the synthesis of cyclic GMP was fundamental for the control of essential parasite processes (16). cGMP activates the enzyme protein kinase G (PKG) which was proposed to regulate a phosphoinositide phospholipase C (PI-PLC) that produces inositol-1,4,5-trisphosphate (IP_3) which would act on an unidentified channel in the ER allowing the release of Ca^{2+} into the cytosol (17). However, the role of Ca^{2+} itself was not considered in this hypothetical signaling cascade. Ca^{2+} is a known modulator of Ca^{2+} channels (18) and it is known that the activation of PI-PLC depends on the local $[Ca^{2+}]_{cyt}$ (19, 20). In this work we characterized the role of intracellular signaling in Ca^{2+} entry at the plasma membrane and we present a model for crosstalk between cGMP and cytosolic Ca^{2+} for the activation of *T. gondii*'s lytic cycle traits.

RESULTS

Ca^{2+} entry at the plasma membrane

We assessed Ca^{2+} entry (Fig. 1A) in Fura 2-loaded extracellular tachyzoites by adding Ca^{2+} to *T. gondii* tachyzoites in suspension in a low Ca^{2+} buffer (EGTA buffer) (100 µM EGTA, ~30 nM free $[Ca^{2+}]_{ext}$). Fig. S1A shows the loading protocol used, described in detail in the experimental procedures section, and Fig. 1A shows a control trace highlighting what we defined as "Basal Ca^{2+} entry" (*pink arrow*). An increase in fluorescence indicates increase of cytosolic Ca^{2+} resulting from influx from the extracellular milieu (Fig. 1A, *basal Ca^{2+} entry*). The rate of increase ($\Delta[Ca^{2+}]$/sec) increased with the concentration of extracellular Ca^{2+} (Fig. S1B). This result indicated that extracellular tachyzoites express Ca^{2+} channels at the plasma membrane (PM) that are either activated by extracellular Ca^{2+} or the electrochemical gradient allows the flow of Ca^{2+} in through an open channel. The peak of cytosolic Ca^{2+} after the initial increase is followed by a recovery phase (due to uptake by other stores or extrusion) and a stabilization of the cytosolic concentration within nM range (Fig. 1A, *recovery*). This stable concentration is likely the result of an equilibrium between Ca^{2+} entry through the PM channels and the compensatory action of the PM and endoplasmic reticulum (ER) Ca^{2+} ATPases, that actively remove Ca^{2+} from the cytosol.

Ca^{2+} entry and pumping into intracellular stores is essential for keeping stores replenished. To examine the relationship between the ER, the largest intracellular store in cells (21), and Ca^{2+} entry, we manipulated the extracellular Ca^{2+} concentration. We found that the rate of Ca^{2+} entry

after adding extracellular Ca^{2+}, was lower when parasites were pre-incubated with 1.8 mM Ca^{2+} (Fig. 1B, *gray trace*) and was faster if they were pre-incubated with EGTA (100 µM) (Fig. 1B, *light blue trace*). We next analyzed the rate of Ca^{2+} entry in parasites pre-exposed to EGTA buffer by various lengths of time. The longer the parasites stayed in the EGTA buffer, the faster was the rate of influx, $\Delta[Ca^{2+}]_i$/sec, upon addition of extracellular Ca^{2+} (Fig 1C). This could be the result of stores becoming depleted with the longer incubation in EGTA buffer, which could trigger a higher rate of PM Ca^{2+} entry.

In *T. gondii*, Ca^{2+} uptake into the ER is actively mobilized by the Sarco/endoplasmic reticulum Ca^{2+} ATPase (SERCA) homologue (TgSERCA) which, as in other eukaryotes, is sensitive to the SERCA inhibitor, thapsigargin (TG) (22, 23). Inhibition of SERCA by TG resulted in an increase of cytosolic Ca^{2+} due to the ER constitutive efflux/leakage pathway (Fig. 1D, *TG-triggered Ca^{2+} increase*). We observed that addition of extracellular Ca^{2+} to suspensions previously exposed to TG resulted in enhanced Ca^{2+} entry, which could be due to a store filling requirement or regulation by cytosolic Ca^{2+}. The cytosolic increase is followed by a recovery phase (Fig. 1D). To assess the contribution of the TG-triggered cytosolic Ca^{2+} increase to the stimulation of calcium entry we quantified Ca^{2+} entry after the addition of various concentrations of TG. The rate of Ca^{2+} entry, ($\Delta[Ca^{2+}]_i$/sec) was higher when adding Ca^{2+} after 1 µM TG (Fig. S1C). The rate of TG-triggered cytosolic Ca^{2+} ($\Delta[Ca^{2+}]$/sec), showed correlation with the concentration of TG added (Fig. S1D). However, the cytosolic Ca^{2+} increase ($\Delta[Ca^{2+}]$) only showed significance between 0.5 and 2 µM TG (Fig. S1E). In a similar experiment but in the presence of extracellular Ca^{2+} the rate and amplitude of cytosolic Ca^{2+} increase triggered by TG was dramatically increased (Fig. S1F, G & H). However, the rate of Ca^{2+} entry was significantly lower with higher concentrations of TG (Fig. S1F, *bar graph*). This slower response could be because of the stores being fully replenished or could be an off-target effect of the higher concentration of TG (24). More experiments are needed to clarify the link between the filling state of the stores and its communication with the PM entry mechanism.

The cytosolic Ca^{2+} increase triggered by addition of TG was significantly higher in cells preincubated in 1.8 mM extracellular Ca^{2+} compared to cells suspended in an EGTA buffer (~30 nM extracellular Ca^{2+} calculated with maxchelator) (Fig. 1E, *compare gray and blue traces*). This could be because of increased Ca^{2+} entry or because of higher ER Ca^{2+} stored or a combination of both. To highlight Ca^{2+} entry we added 1.8 mM BAPTA prior to TG to block extracellular Ca^{2+},

which resulted in a reduction of the TG-triggered cytosolic increase (Fig. 1F, *red trace*), indicating that the difference between plus and minus extracellular BAPTA is due to Ca^{2+} entry.

The concentration of cytosolic Ca^{2+} is the result of Ca^{2+} influx through the PM and the pumping of Ca^{2+} out by PMCA or into the ER by SERCA. To underline the PMCA's role in regulating cytosolic Ca^{2+}, we blocked the flow of Ca^{2+} entry by adding BAPTA a few seconds after adding extracellular Ca^{2+}. We saw a sharp decrease in cytosolic Ca^{2+} after the addition of BAPTA followed by steady state of cytosolic calcium (Fig. 1G). We attributed this effect to the action of the PMCA as BAPTA prevented extracellular Ca^{2+} to re-enter the cytosol, which was masking the pumping activity. This sharp decrease was also seen when adding BAPTA after Ca^{2+} in the presence of TG (Fig. 1H) to block the contribution of the ER. Further demonstration for the role of the PMCA was shown by pre-incubating parasites with vanadate, an inhibitor of P-type ATPases (Fig. 1I), which resulted in a higher rate of Ca^{2+} entry demonstrating the activity of the enzyme in maintaining cytosolic Ca^{2+} at physiological levels. The $\Delta[Ca^{2+}]$ between the peak and the baseline reached with BAPTA represent the amount of Ca^{2+} that is pumped out by the action of the PMCA, which is approximately 35% and 45% of the cytosolic Ca^{2+} rise after adding Ca^{2+} with and without TG respectively (Fig. 1G-H). Ca^{2+} was extruded from the cytosol at a rate similar to the rate seen in cells pre-treated with TG, supporting a more important role for the PM Ca^{2+} pump over SERCA in maintaining cytosolic Ca^{2+}. This result supports the housekeeping role of PMCA as described for other PMCAs (25, 26).

In summary, these data showed the presence of Ca^{2+} channels at the PM that permeates Ca^{2+} and that are compensated by the action of a plasma membrane Ca^{2+} pump to maintain cytosolic Ca^{2+} homeostasis (27, 28). In addition, depletion of intracellular Ca^{2+} by either incubating the cells with extracellular EGTA or BAPTA, or by inhibition of SERCA stimulated Ca^{2+} influx (enhanced Ca^{2+} entry).

Ca^{2+} entry pathways with distinct Ca^{2+} affinities and blocker's sensitivities

With the aim of further characterizing the channel(s) responsible for PM Ca^{2+} entry, Fura 2-loaded tachyzoites in suspension in EGTA buffer were exposed to varying concentrations of extracellular Ca^{2+} (Fig. S2A and 2A). We measured the peak cytosolic Ca^{2+} and found that it increased with the concentration of extracellular Ca^{2+} added to the suspension in a biphasic shape (Fig 2A). This pattern indicated the presence of more than one type of Ca^{2+} channel for influx with

at least two different affinities for Ca^{2+} (Fig. 2A). We next examined the effect of known mammalian Ca^{2+} channel blockers like nifedipine, cilnidipine, verapamil (29), or anthranilic acid (ACA) (30), a wide spectrum transient receptor potential (TRP) channel inhibitor, on the ΔCa^{2+} following addition of extracellular Ca^{2+}. Inhibition by 100 µM Verapamil, a phenylalkylamine, was ~40% and no inhibition was observed with diltiazem a benzothiazepine type Voltage Dependent Calcium Channel (VDCC) antagonist (Table 1). Dihydropyridines, known blockers of L–type VDCC like nifedipine and cilnidipine, were highly effective and blocked Ca^{2+} influx at ~80% and ~75% respectively (Table 1). Interestingly, ACA inhibited Ca^{2+} influx by approximately 50% (Table 1). Since dihydropyridines and ACA block different types of channels, we next tested these inhibitors at varying concentrations of extracellular Ca^{2+}. At 250 µM extracellular Ca^{2+}, nifedipine blocked entry almost ~100% (Fig. 2B-C, Table 2) while at higher concentrations of extracellular Ca^{2+} (1.8 mM) a residual ~20% activity of Ca^{2+} influx was detected (Table 2). This result indicated that at high concentrations of extracellular Ca^{2+}, the partial inhibition is due to the activity of more than one Ca^{2+} channel while at lower extracellular Ca^{2+} the nifedipine-sensitive channel appeared to be the main active channel. On the other hand, ACA, inhibited Ca^{2+} entry by ~50% at all tested extracellular [Ca^{2+}] (Fig. 2D-E). The combination of both nifedipine and ACA resulted in an additive inhibition of Ca^{2+} entry, as most likely they block different channels (Fig. 2F). Taken together these results supported the presence of more than one type of Ca^{2+} channel with different affinities for Ca^{2+} and inhibited by different types of blockers.

We previously showed that cytosolic Ca^{2+} itself could modulate/activate one of the Ca^{2+} channels at the PM (12). With the aim to highlight this activity of Ca^{2+} entry at the PM we pre-loaded *T. gondii* tachyzoites with BAPTA-AM to chelate cytosolic Ca^{2+} (iBAPTA). Under these conditions the "basal Ca^{2+} entry" was significantly reduced as shown after adding extracellular Ca^{2+} (Fig. 2G and H). Interestingly, under these conditions, nifedipine blocked Ca^{2+} entry by 100% (Fig. 2G) while ACA inhibited the usual 50% (Fig. 2H,-I-J). This result showed that chelating intracellular Ca^{2+} inhibited Ca^{2+} entry and this inhibition was complete when combined with nifedipine in support for the presence of at least two Ca^{2+} entry pathways (one sensitive to nifedipine and one modulated by cytosolic Ca^{2+}). We believe that the residual activity observed in the presence of ACA or iBAPTA is due most likely to Ca^{2+} influx through the nifedipine-sensitive channel (Fig. 2H-I-J).

We also studied constitutive Ca^{2+} influx which was observed in extracellular tachyzoites when exposed to 1.8 mM extracellular Ca^{2+}. This is evidenced by a steady increase of cytosolic Ca^{2+} over time, which is not observed when the parasites are suspended in EGTA buffer (Fig. S2B). ACA inhibited this activity almost 100% while nifedipine showed only a minor effect (Fig S2B). This result showed that at least one of the PM channels was leaky, as it allowed constitutive Ca^{2+} influx, and it was sensitive to ACA but not to nifedipine.

Overall Ca^{2+} influx in extracellular tachyzoites of *T. gondii* is occurring through at least two different types of channels; one channel sensitive to nifedipine with higher affinity for Ca^{2+} (VDCC-like channel) and a channel with lower affinity for Ca^{2+}, sensitive to ACA and modulated by cytosolic Ca^{2+} (TRP-like channel).

The role of cGMP signaling in Ca^{2+} entry

With the aim to further characterize Ca^{2+} entry activated by cytosolic Ca^{2+}, we tested Zaprinast, a cGMP phosphodiesterase inhibitor (Fig. 3A), known to increase cytosolic Ca^{2+} (31). We observed that Ca^{2+} entry was significantly increased after stimulation with Zaprinast (Fig. 3B, *violet trace*) compared to the control rate of entry (Fig. 3B, *blue trace, no previous additions*). As the cytosolic Ca^{2+} decreases after the peak ensuing from the addition of Zaprinast (recovery phase) (Fig. S3A), we added Ca^{2+} at different times after the peak and found that the magnitude of Ca^{2+} entry decreased as the cytosolic Ca^{2+} decreased (Fig. S3A). Adding Zaprinast in the presence of extracellular Ca^{2+} resulted in a cytosolic increase from a combination of release from stores and Ca^{2+} entry through the PM (Fig. 3C, *brown trace*). We demonstrated this by adding extracellular BAPTA (free acid) right before adding Zaprinast which would not allow for Ca^{2+} to enter (Fig. 3C, *green trace*), resulting in a diminished cytosolic Ca^{2+} peak indicating that the difference between both conditions (with and without BAPTA) is due to Ca^{2+} entry (Fig. 3C, *green trace*). This difference is not found in the control experiments done in the absence of extracellular Ca^{2+} (Fig S3B).

We next tested nifedipine which inhibited Ca^{2+} entry by ~80% (Fig. 3D, *orange trace, Ca^{2+} was added 300 sec after Zaprinast*). Note that nifedipine did not inhibit the Zaprinast stimulation of calcium release from intracellular stores, as it was acting only on the plasma membrane channel. Addition of ACA inhibited Ca^{2+} entry by ~50% (Fig 3E) and did not impact the Zaprinast-stimulated calcium release. Interestingly, when testing nifedipine in the presence of extracellular

Ca^{2+}, a condition in which the stores are filled, Ca^{2+} entry stimulated by Zaprinast was insensitive to nifedipine (Fig 3F) while ACA inhibited ~70% of the entry (Fig 3G). This result indicated that the PM Ca^{2+} entry channel activated by the signaling pathway triggered by Zaprinast is nifedipine insensitive but can still be inhibited by ACA. Note that the inhibition of Ca^{2+} entry observed in Fig 3D and 3E is measured after recovery of cytosolic Ca^{2+}.

To better understand the interplay between cGMP and Ca^{2+} entry, we added a permeable version of cGMP to a suspension of Fura 2-loaded parasites in EGTA buffer, which resulted in an increase in cytosolic Ca^{2+} most likely from intracellular stores. Addition of extracellular Ca^{2+} after cGMP, resulted in enhanced Ca^{2+} entry (Fig. 4A, *green trace*). cGMP activates the enzyme protein kinase G (PKG) and to ensure that the effect of cGMP was through PKG we pre-incubated the parasite suspensions with compound 1 (Cpd1), a specific inhibitor of PKG (32). The cytosolic enhanced Ca^{2+} entry stimulated by cGMP was suppressed by Cpd1, supporting a role for PKG (Figs 4A, *grey trace*). The basal Ca^{2+} entry was slightly affected by Cpd1 (Fig 4 B-C, *compare red and blue traces and bars after adding* Ca^{2+}*).* However, the enhanced Ca^{2+} entry was fully inhibited (Fig. 4C, *compare green and gray bars*).

To further examine the role of PKG in Ca^{2+} entry, we tested a PKG mutant that is insensitive to Cpd1 (PKGM) and its counterpart PKGT (sensitive to Cpd1). PKGM and PKGT are genetically modified strains in which the PKG gene was replaced by a Ty-tagged allele harboring either the wild-type gatekeeper (PKGT) or a $T^{761}M$ mutation (PKGM) (31). Change of the PKG$T^{761}M$ residue at the base of the ATP binding pocket made PKG refractory to Cpd1 inhibition. The PKGM mutant was insensitive to growth inhibition by Cpd1 while the PKGT was sensitive (Fig. S4A). Consistent with the growth result, the PKGT mutant showed reduced basal Ca^{2+} entry by 60% in the presence of Cpd1 (Fig. 4D, *maroon trace and bar*) and enhanced Ca^{2+} entry induced by cGMP was inhibited by ~75% (Fig. 4E, *maroon trace and bar*). Cpd1 did not inhibit basal Ca^{2+} entry in the PKGM mutant (Fig. 4F), or the cGMP mediated Ca^{2+} release followed by enhanced Ca^{2+} entry (Fig. 4G). In summary, we showed that the mechanism of Ca^{2+} entry enhanced by cytosolic Ca^{2+} is linked to a signaling pathway in which PKG forms part of.

The role of the phosphatidyl inositol phospholipase C in Ca^{2+} ***entry***

It has been proposed that the role of PKG in Ca^{2+} signaling could be through its regulation of PI-PLC (33) (Fig. 5A). To test the potential role of PI-PLC in Ca^{2+} entry we used the inhibitor

U73122 and its inactive analog U73343 (34, 35) (Fig. S4B, *inhibitor effect on growth*). Pre-incubation with the inhibitor blocked the effect of cGMP on intracellular Ca^{2+} and significantly decreased Ca^{2+} entry after the addition of extracellular Ca^{2+} (Fig. 5B, *brown trace*). Pre-incubation with the inactive analogue, however, resulted in Ca^{2+} responses indistinguishable from the control (Fig. 5B, *gray trace*). Interestingly, parasites incubated with U73122 and nifedipine, blocking both potential routes of Ca^{2+} influx, showed 100% inhibition of Ca^{2+} entry (Fig 5C, *orange trace*) further substantiating the presence of at least two pathways responsible for Ca^{2+} entry.

To further characterize the role of PI-PLC in Ca^{2+} entry, we tested the conditional mutant for PI-PLC, *iΔPIPLC*, in which the expression of the PI-PLC gene is regulated by anhydrotetracycline (ATc) (36). We cultured the mutant in the presence of ATc (+ATc) and compared Ca^{2+} entry with the same mutant grown without ATc (-ATc). The basal Ca^{2+} entry without any stimulation was comparable between +ATc and -ATc parasites (Fig 5D). We next looked at the enhanced Ca^{2+} entry by adding TG followed by extracellular Ca^{2+}. Downregulation of PI-PLC almost entirely abolished the enhanced Ca^{2+} entry and the activity observed was similar to the basal Ca^{2+} entry (Fig. 5E). Quantifications are shown in part F. Most interestingly, the Zaprinast stimulated cytosolic Ca^{2+} influx was highly reduced in the *iΔPIPLC* (+ATc) mutant and resulted in diminished Ca^{2+} stimulated Ca^{2+} entry (Fig 5G). This result supports the involvement of PI-PLC in the pathway stimulated by Zaprinast on intracellular stores and places PI-PLC as an important player in the Ca^{2+} activated Ca^{2+} entry (or enhanced Ca^{2+} entry).

We tested the effect of U73122 on the *iΔPIPLC* (+ATc) mutant and showed that they were insensitive as no effect on Ca^{2+} entry was observed upon extracellular Ca^{2+} addition (Fig. 5H, *pink trace, compare with the pink trace in part D*). The inactive analog, U73343, however, produced a similar response on the *iΔPIPLC* mutant cultured with or without ATc (Fig. 5I). The basal Ca^{2+} entry of the *iΔPIPLC* (+ATc) mutant was sensitive to nifedipine at the same level as the parental line indicating that basal Ca^{2+} entry is the result of at least two activities (Fig 5J, *gray trace*). Enhanced Ca^{2+} entry stimulated by cGMP was also significantly diminished in the *ΔPIPLC* (+ATc) mutant (Fig. 5K, *pink trace*) and if pre-incubated with nifedipine resulted in ~100% inhibition because both pathways of Ca^{2+} influx were blocked (Fig. 5K, *dotted pink trace*). These results supported the participation of PI-PLC in a Ca^{2+} entry pathway modulated by cytosolic Ca^{2+} through PKG. The enhanced Ca^{2+} entry would be the combination of the basal Ca^{2+} entry and the Ca^{2+} influx induced by PKG and PI-PLC.

In summary, our results showed that Ca^{2+} entry through an ACA sensitive channel is modulated by Ca^{2+} through a signaling pathway that involves cGMP, PKG and PIPLC.

Ca^{2+} entry and the lytic cycle

Intracellular tachyzoites replicate inside a porous vacuole which is in equilibrium with the host cytosol where the concentration of Ca^{2+} is ~100 nM. Under these conditions, parasites can take up Ca^{2+}, during physiological host Ca^{2+} fluctuations, which are also impacted by extracellular Ca^{2+} (11). We investigated if the extracellular Ca^{2+} in the culture would influence parasite growth. We measured *T. gondii* growth using plaque assays and varied the concentration of extracellular Ca^{2+}. Parasites engage in repetitive cycles of invasion, replication, and egress causing host cell lysis and formation of plaques are observed as white spots after staining with crystal violet. Plaque sizes were measured in cultures with 1.8, 0.5 and 0.25 mM extracellular Ca^{2+} after 8 days of growth and, interestingly, we found that plaques were smaller at lower concentrations of Ca^{2+} (Fig. 6A). This result indicated that intracellular tachyzoite growth is impacted by the extracellular Ca^{2+} conditions. Non-infected host cells grew normally under similar conditions although they did not grow in the absence of Ca^{2+} (Fig. S5A and *not shown*).

We next investigated growth inhibition by nifedipine, cilnidipine, ACA and Cpd1 at the concentrations we observed inhibited Ca^{2+} influx, 10 µM, 40 µM, 1 µM and 1 µM respectively. Nifedipine did not inhibit growth, most likely due to the poor stability of the compound in cultures (Fig. 6B). Nifedipine solutions are extremely unstable and photosensitive, and rapidly degrades at 25^{o}C, and the concentration declines to about 90% within six hours (Sigma product information). Plaques formed in the presence of ACA were significantly smaller, indicating that Ca^{2+} influx mediated by the TRP-like channel is important for parasite growth. No plaques formed when incubated with Cpd1, a stronger inhibition than the one observed with ACA due to other essential roles of PKG. Ca^{2+} influx through a channel with pharmacological characteristic of a VDCC is important as shown by the lack of plaques in the presence of cilnidipine. Non-infected host cells controls showed no toxicity when grown in the presence of the inhibitors at similar concentrations (Fig. S5B). However, U73122 showed a minor effect in the integrity of the host cell monolayer (Fig. S5B).

We next determined the EC_{50} (concentration of drug needed to inhibit growth by 50%) of cilnidipine, ACA, and other inhibitors (Table 3). Cilnidipine EC_{50} was 10 times lower than the

effective concentration for inhibiting Ca^{2+} influx, which suggests an additional target. Verapamil showed a modest effect with an EC_{50} of ~31 µM. ACA was highly effective with an EC_{50} of 1.6 µM. The EC_{50} for the PIPLC inhibitor U723122 was 0.35 µM and the inactive analog, U73343 was less effective with an EC_{50} of 2.4 µM. This result was consistent with the specific PI-PLC inhibition properties of both compounds (Table 3). We also tested invasion and attachment and observed inhibition by nifedipine, but no effect was observed with cilnidipine (Fig. 6C). Reduced invasion and increased attachment were also observed in the presence of Zaprinast or U73122 (Fig. 6C). The U73122 showed a stronger inhibition of invasion than its inactive analog U73343 (Fig. 6C), consistent with the growth inhibition.

To further characterize Ca^{2+} influx during egress we used pharmacological inhibition of the potential Ca^{2+} entry channels and measured time to egress and quantified fluorescence fluctuations of tachyzoites expressing the genetically encoded calcium indicator, GCaMP6f (Fig. S7A). The experimental strategy was to permeabilize the host cell with a very low concentration of saponin (0.01%), added 1 min after the start of the recording, which will expose the PVs to either high (1.8 mM) or low (~30 nM) extracellular Ca^{2+}. Under these conditions egress is stimulated as we previously demonstrated (11). Previously, we showed that two peaks of cytosolic Ca^{2+} preceded egress: the first peak originating from intracellular stores followed by a second peak associated with Ca^{2+} influx. This Ca^{2+} influx was sensitive to nifedipine (11). Interestingly, at low extracellular Ca^{2+}, ACA significantly delayed parasite egress by affecting the first peak (Fig. 7A, *EGTA*), while at high extracellular Ca^{2+} there was no difference in Ca^{2+} fluctuations or time of parasites to egress (Fig 7B, *high* Ca^{2+}). We showed previously that ACA targets the TgTRPPL-2 channel, which localizes to the PM and the ER of *T. gondii* (12). Deletion of TgTRPPL-2 decreased both ER calcium efflux and Ca^{2+} entry. Since ACA targets both ER and PM localized TgTRPPL-2, it would explain the delayed egress observed in the EGTA buffer. When stimulating with Zaprinast, ACA did not affect time of egress at low or high extracellular Ca^{2+} (Fig. S7A-B). This could be because Zaprinast alone can sustain the Ca^{2+} threshold needed to stimulate egress. However, at high extracellular Ca^{2+}, ACA produced a modest shift of the first peak of cytosolic Ca^{2+} oscillation which was not statistically different (Fig. S7B).

Finally, we examined the effect of Ca^{2+} inhibitors on parasite motility. We evaluated the relative distance traveled by parasites before and after addition of 1.8 mM Ca^{2+} (Fig. S6B). Using a cell-tracking algorithm (37) and GCaMP6f-expressing parasites we were able to confirm that

extracellular Ca^{2+} enhances motility and this stimulation was inhibited by nifedipine, cilnedipine or ACA evaluated as the distance traveled by the parasite (Fig. 7C). Next, we tested parasite motility stimulated by Zaprinast. We monitored distance traveled in low (Fig. 7D) and high (Fig. 7E) extracellular Ca^{2+} in the presence or absence of the inhibitors: nifedipine, ACA or Cpd1. This experiment showed that inhibition of PKG by Cpd1 also diminished parasite motility at low and high extracellular Ca^{2+}. Interestingly, motility was inhibited by ACA at low extracellular Ca^{2+}, but not at high extracellular Ca^{2+}. At low extracellular Ca^{2+} motility is likely triggered by intracellular store release and the effect of ACA at low Ca^{2+} could be the result of its inhibition of the ER Ca^{2+} leak (TgTRPPL-2). As the concentration of extracellular Ca^{2+} is low the low affinity channel is likely non-functional so ACA would be irrelevant. When the extracellular Ca^{2+} is high, ACA has no effect as most likely Ca^{2+} is still able to enter the parasite through the high affinity channel.

DISCUSSION

An increase of cytosolic Ca^{2+} in cells is the result of influx from the extracellular milieu through the plasma membrane (PM) and/or release from intracellular stores mainly from the ER. The resting cytosolic Ca^{2+} is highly regulated and PM Ca^{2+} ATPases (PMCA) play an essential role by pumping excess cytosolic Ca^{2+} out of the cell (25). The ER Ca^{2+} reuptake is performed by the SERCA Ca^{2+} pump that controls the ER luminal [Ca^{2+}]. A poorly defined Ca^{2+} leak in the ER protects the organelle against Ca^{2+} overload. However, this constitutive Ca^{2+} leak combined with other mechanisms at the PM like the PMCA, would result in a continuous loss of stored Ca^{2+} from the organelles if a mechanism of entry at the PM would not be present (38).

In *T. gondii*, both intracellular (11) and extracellular parasites (10) use Ca^{2+} influx for replenishing intracellular stores, or for enhancing invasion and motility traits, respectively. The increase of cytosolic Ca^{2+} resulting from both extracellular and/or intracellular influx can contribute to the activation of downstream signaling pathways that promote progression through the parasite's lytic cycle. Ca^{2+} entry from the extracellular milieu would be the only logical mechanism by which intracellular and extracellular parasites can replenish their intracellular stores which are essential for signaling and lytic cycle progress. However, the mechanisms of Ca^{2+} entry are poorly understood, and few molecular players have been identified.

In this work we focused on Ca^{2+} entry in extracellular tachyzoites, and we distinguish the basal entry that is observed right after adding extracellular Ca^{2+} (1.8 mM Ca^{2+}) to parasites previously

suspended in a low extracellular buffer (100 μM EGTA, ~30 nM free Ca^{2+}) from the enhanced entry observed after an increase of cytosolic Ca^{2+} triggered by TG, Zaprinast or cGMP (Ca^{2+} activated Ca^{2+} entry or CACE). This enhanced entry could also be the result of store regulation although previous results did not support the presence of this mechanism (10). We showed that more than one type of PM channel is most likely functional in extracellular tachyzoites of *T. gondii* with different affinities for Ca^{2+} and different pharmacological profiles. Our hypothesis is that these channels will become functional or activated by specific triggers that would allow them to open at specific points during the lytic cycle of the parasite. Ca^{2+} entry can be inhibited by VDCC blockers like nifedipine and cilnidipine and these inhibitors, block Ca^{2+} entry by 80-85% at high extracellular Ca^{2+} (> 1.5 mM Ca^{2+}) and ~100% at lower extracellular Ca^{2+} (< 250 μM Ca^{2+}). This inhibition pattern stressed the functioning of a second channel at high extracellular Ca^{2+} concentrations.

In this work we described the regulation of a PM Ca^{2+} entry activity by Ca^{2+} itself through a signaling pathway that involves cGMP, PKG and PI-PLC. This activity was sensitive to the broad spectrum TRP channel blocker ACA, supporting that the target of this drug is the previously described TgTRPPL-2 (12). TgTRPPL-2 localized to the plasma membrane and the ER, was found to conduct Ca^{2+}, and was inhibited by ACA and benzamil. TgTRPPL-2 mutants showed reduced Ca^{2+} influx, a phenotype like the one resulting from ACA inhibition.

The processes of invasion and egress are highly regulated, dynamic, and essential for the propagation of the *T. gondii* infection. Each step of the parasite lytic cycle is precise, fast, and efficient with distinct and interrelated molecular processes occurring in a coordinated manner and each step is preceded by an increase of cytosolic Ca^{2+} (4, 5). The extracellular motile tachyzoite is surrounded by the high Ca^{2+} concentration of the extracellular milieu (>1.5 mM) and we previously demonstrated Ca^{2+} influx under these conditions, which occurred in a regulated fashion (10). Keeping intracellular Ca^{2+} stores (like the ER) replenished in replicating intracellular *T. gondii* is essential for the continuation of the parasite's lytic cycle as exit from the host cell is preceded by a rapid required increase of the parasite's cytosolic Ca^{2+} (9). Replicating tachyzoites (the fast-growing form of *T. gondii*) are sequestered in a porous PV that is in equilibrium with the innately low Ca^{2+} (<100 nM) environment of the host's cytosol. This fluctuates during natural Ca^{2+} signaling events and could reach low μM levels (39) globally, or higher levels at membrane contact sites (MCS) (39). We showed that these transient increases in host cytosolic Ca^{2+} were followed

invariably by Ca^{2+} increase in the PV followed by Ca^{2+} entry into the parasite cytosol (11). This previous work demonstrated the functionality of PM mediated Ca^{2+} entry in intracellular replicating tachyzoites. Host cytosolic Ca^{2+} oscillations were followed by Ca^{2+} entry into the parasite cytosol triggering oscillations where the Ca^{2+} drop would be due (in part) to pumping of Ca^{2+} by the SERCA-Ca^{2+} ATPase into the ER. This Ca^{2+} stockpile in the parasite ER is essential for egress as we showed that a threshold for cytosolic Ca^{2+} had to be attained for successful egress as cytosolic increases that do not reach the threshold resulted in oscillations without egress (11). Interestingly, we found that growing parasites in lower extracellular Ca^{2+} resulted in smaller plaques supporting the relevance of host cytosolic fluctuations for replenishment of tachyzoite intracellular Ca^{2+} stores. We also showed that inhibiting the signaling pathway that leads to enhanced Ca^{2+} entry inhibited *T. gondii* growth.

We hypothesize that PM Ca^{2+} channels functionally active in intracellular parasites are likely different than the ones that become active in extracellular parasites. The PM Ca^{2+} channels functioning at relatively low levels of extracellular Ca^{2+} (high µM levels) (nifedipine sensitive) supported Ca^{2+} entry in intracellular tachyzoites during normal host calcium fluxes. Ca^{2+} would be captured in the parasite ER to be released through an unknown ER channel. An ER Ca^{2+} leak would protect the ER from Ca^{2+} overload and contribute to the filling of other stores. Upon egress, tachyzoites are in contact with the high Ca^{2+} concentration of the extracellular milieu (>1.5 mM) and PM Ca^{2+} entry in this environment could be through a different type of channel, like the TRP-like channel that our lab characterized (Fig. 8). This PM Ca^{2+} entry in extracellular tachyzoites would maintain parasite motility until they invade a new host cell and begin the replication process anew.

The cyclic nucleotide cGMP is an essential signaling molecule in apicomplexan parasites (32, 40-45) and the enzyme that synthesizes it, Guanylyl Cyclase (TgGC), is essential (16). TgGC is a large, 22 transmembrane span protein with a predicted mass of 477 kDa that accumulates at the apical cap region of the plasma membrane of *T. gondii*. Conditional knockdown approaches demonstrated that TgGC is essential for tachyzoite cell-to-cell transmission by regulating egress, migration, and invasion (16, 17, 46). The essentiality of TgGC was also established in an *in vivo* model of toxoplasmosis, where parasites lacking TgGC were incapable of producing lethal infection in highly sensitive C57Bl/6 mice due to defects in proliferation, dissemination, and persistence (16).

Increase of cGMP levels induces PKG activation which mobilizes intracellular Ca^{2+} presumable through the activation of PI-PLC that hydrolyzes PIP_2 and produces IP_3 and DAG (47). IP_3 would open an unidentified channel in the ER to release Ca^{2+} into the cytosol. Previous PKG dependent phosphoproteome from *P. falciparum* (48) and the most recent phosphoproteome from *T. gondii*, position PI-PLC as a possible phosphorylation substrate of PKG (49). In an additional study with ookinetes of *P. bergei*, inhibition of PKG did not result in $PI(4,5)P_2$ accumulation as could be expected if PKG is activating PI-PLC (50). In this study it was observed that the phosphoinositide-metabolizing enzymes were less phosphorylated when PKG was inhibited. In addition, lipidomic analysis of total extracts revealed that Zaprinast triggered PIP, PIP_2 and PIP_3 depletion (50), indicating PI-PLC activation. More studies are necessary to establish that PI-PLC is a direct target of PKG.

Our present work showed that cGMP is involved in the Ca^{2+} regulation of Ca^{2+} entry as we showed the participation of PKG and PI-PLC in a cascade of molecular events that culminates in the stimulation of Ca^{2+} influx. Increase of cytosolic levels of cGMP induced by the inhibition of PDEs by Zaprinast or by the addition of a permeable cGMP, resulted in enhanced Ca^{2+} entry that was diminished when PKG or PI-PLC were pharmacologically or genetically ablated. Cytosolic Ca^{2+} increase stimulated by cGMP was significantly reduced upon PI-PLC inhibition, indicating that PKG acts upstream to PI-PLC and could be required for PI-PLC activation. However, PI-PLC requires Ca^{2+} for activity (47), which adds complexity to the proposed signaling cascade: cGMP---PKG---PI-PLC---Ca^{2+} release from intracellular stores---stimulation of Ca^{2+} entry. Is cGMP acting on a Ca^{2+} influx channel (ER or PM) directly and is this initial Ca^{2+} influx contributing to the stimulation of PI-PLC and enhanced Ca^{2+} entry? Addition of cGMP resulted in cytosolic Ca^{2+} increase which could be a combination of its effect in PI-PLC stimulation plus its direct effect in a Ca^{2+} channel. This could explain the residual activity observed in cytosolic Ca^{2+} after adding cGMP to cells previously incubated with a PI-PLC inhibitor or cells in which PI-PLC was downregulated.

In summary, a cytosolic Ca^{2+} increase is important not only for activating Ca^{2+} entry but also is essential for activating PI-PLC as this enzyme has very little activity without Ca^{2+} (47). Most likely a crosstalk between the cytosolic Ca^{2+} influx mechanisms and release from intracellular stores intersects at the PI-PLC. Interestingly, ~100% inhibition of Ca^{2+} entry was achieved at high extracellular Ca^{2+} concentrations with nifedipine combined with inhibitors of the phosphoinositide

phospholipase C. Ca^{2+} entry should be considered as an essential component of the signaling cascades that precede the stimulation of *T. gondii* biological features.

EXPERIMENTAL PROCEDURES

Chemical and reagents - All reagents used were of high analytical grade. Calcium reagents like Fura 2-AM, BAPTA-AM, BAPTA, etc were from AAT Bioquest.

Cell culture and strains - All parasite strains were maintained in human telomerase reverse transcriptase immortalized foreskin fibroblasts (hTERT) (51) grown in Dulbecco's modified minimal essential media (DMEM) with 1% FBS, and streptomycin-penicillin (1:100) (Corning) and regularly tested and treated for Mycoplasma.

Cytosolic calcium measurements with FURA-2 – T. gondii tachyzoites were loaded with Fura 2-AM as previously described (22, 52). Briefly, freshly released tachyzoites were washed twice with buffer A plus glucose (BAG; 116 mM NaCl, 5.4 mM KCl, 0.8 mM $MgSO_4$, 50 mM Hepes, pH 7.3, and 5.5 mM glucose), by centrifugation (706 x *g* for 10 min) and re-suspended to a final density of 1 x $l0^9$ parasites/ml in loading buffer (BAG plus 1.5% sucrose, and 5 μM Fura 2-AM). The suspension was incubated for 26 min at 26 °C with mild agitation. Subsequently, the parasites were washed twice (2000 x *g* for 2 min) with BAG to remove extracellular dye, re-suspended to a final density of $1x10^9$ parasites per ml in BAG and kept in ice. Parasites are viable for a few hours under these conditions. For fluorescence measurements, 2 x 10^7 parasites/mL were placed in a cuvette with 2.5 mL of Ringer's buffer without calcium (155 mM NaCl, 3 mM KCl, 1 mM $MgCl_2$, 3 mM NaH_2PO_4, and 10 mM Hepes, and 10 mM dextrose). Fluorescence measurements were done in a Hitachi F-7000 fluorescence spectrofluorometer using the Fura 2 conditions for excitation (340 and 380 nm) and emission (510 nm). The Fura 2 fluorescence response to Ca^{2+} was calibrated from the ratio of 340/380 nm fluorescence values after subtraction of the background fluorescence of the cells at 340 and 380 nm as described previously (53). The rate of Ca^{2+} increase following the addition of Ca^{2+} or inhibitors or agonists, was defined as the change in Ca^{2+} concentration during the initial 20 s after the addition of the reagent. The $\Delta[Ca^{2+}]_i$ was calculated by the difference between the highest peak and basal $[Ca^{2+}]_i$ and recovery was defined as the change of Ca^{2+} concentration after the calcium peak was reached for the subsequent 20 s.

For the experiments with BAPTA-AM *T. gondii* tachyzoites were incubated in loading buffer with 100 μM BAPTA-AM for 20 minutes at room temperature in a rotary mixer, followed by washing 2 times with ringer buffer.

The concentrations of agonists used were: Thapsigargin, 1 μM; Zaprinast, 100 μM; 4-[2-(4-fluorophenyl)-5-(1-methylpiperidine-4-yl)-1H-pyrrol-3-yl]pyridine (Compound 1), 1 μM; 1-[6-[{17β-3-methoxyestra-1,3,5(10)-trien-I7-yl}amino]hexyl]-1H-pyrrole-2,5-dione (U-73122) and 1-[6-[{17β-3-methoxyestra-1,3,5(10)-trien-I7-yl}amino]hexyl]- 1H-pyrrole-2,5 pyrrolidine-dione (U73343), 1 μM; Nifedipine, 10 μM, Anthranilic Acid (ACA), 1 μM; Vanadate, 100 μM;

BAPTA free acid, 1.8 mM; and the permeable form of guanosine 3',5' -cyclic monophosphate 8-bromo- sodium salt (cGMP), 200 μM.

Plaque assays - Plaque assays were performed as previously described (54). Two hundred freshly egressed tachyzoites were used to infect confluent monolayers of hTERT fibroblasts followed by 8 days of growth. Monolayers were fixed and stained with crystal violet and plaque sizes analyzed with FIJI (55) by measuring the area of fifteen plaques per biological replicate. At least 3 biological experiments were done for all conditions testes. Inhibitory compounds were added the first day of the experiment.

Invasion assays - Red-green assays were performed as described (56) with few modifications. Monolayers were infected with 2 x 10^7 freshly lysed parasites for 20 min on ice and then rapidly transferred to 37ºC for 5 min to stimulate invasion. For experiments including inhibitors, these are added 5 min prior to the invasion step. At the end of the invasion step, parasites were fixed with 3% paraformaldehyde. External (attached) parasites were stained with RabbitαSAG1 (gift from John Boothroyd, Stanford University) at a dilution of 1:1000 followed with 1% Triton X-100 permeabilization. Next, labeling of internal parasites (invaded) was done using a MouseαSAG1 dilution 1:200 (MBS312777, MyBioSource.com). Secondary antibodies were goat-αRabbit and Alexa Flour 546 and Alexa Flour 488 goat-αMouse, both used at 1:1,000 dilutions. Images were taken with an Olympus IX-71 inverted fluorescence microscope with a Photometric CoolSnap$_{HQ}$ CCD camera driven by DeltaVision software (Applied Precision, Seattle, WA). Data were compiled from three independent experiments and ten fields of view at 1,000 total magnifications were counted for each experiment. Fields were randomly selected, and parasites counts were made in a blind fashion. Red or green parasites were counted and percentages of each were calculated by dividing for total parasites.

Egress – *GCaMP6f* expressing parasites were used to measure cytosolic calcium fluctuations driving parasite egress as described previously (9). Briefly, glass bottom 35 mm dishes (MatTek Corporation) were used to plate 2 x 10^6 host cells (hTERT) in DMEM supplemented with 10% FBS. After 24 h growth, host cells were infected with 1 × 10^6 *GCaMP6f*-expressing tachyzoites. Twenty-four hours after infection, dishes were washed twice with Ringer buffer plus Calcium (155 mM NaCl, 3 mM KCl, 1 mM MgCl2, 3 mM NaH_2PO4, 10 mM Hepes, pH 7.3, glucose 10 mM and 2 mM $CaCl_2$ or 100 μM EGTA) and parasitophorous vacuoles containing 2 to 8 parasites were observed with an inverted fluorescence microscope (Olympus IX-71). The microscope incubation chamber was set at 37ºC, and live cell imaging was recorded with a CoolSnapHQ CCD camera driven by DeltaVision software (Applied Precision, Seattle, WA). Images were acquired in time-lapse mode with an acquisition rate of 1–2 s during 12 min.

Ringer buffer was used as an extracellular buffer (EB) throughout all video recording. $CaCl_2$ was omitted for experiments done in the absence of extracellular Ca^{2+}, and the media were supplemented with 100 μM EGTA. Anthranilic acid (1 μM) was added in Ringer buffer and preincubated for 5 min before imaging. Egress was stimulated with 0.01% Saponin or 100 μM Zaprinast at 1 min after the initial video recording.

For analysis of the data, mTrackJ, a plugin freely available for Fiji was used to quantify videos (55), and https://imagescience.org/meijering/software/mtrackj/. We compared the Ca^{2+} response (fluorescence tracings of GCaMP6f parasites) and rate of egress post addition of pharmacological drugs.

Motility - We evaluated the role of Ca^{2+} entry and its impact on motility by exposing parasites to Ca^{2+} in the presence of inhibitors, as described previously (9). Briefly, freshly lysed parasites were collected, purified, and plated on 35-mm bottom glass dish pre-treated with 10% FBS. Cells were imaged using a Zeiss LSM 710 confocal microscope set at 37 °C. Then parasites were tracked using a custom-made in-house algorithm (37, 52). The fluorescence of individual parasites (relative cytosolic Ca^{2+}) was compared to the motility of parasites after pharmacological or Ca^{2+} stimulation.

EC_{50} calculation –In vitro growth assays were carried out as described previously using *T. gondii* tachyzoites expressing red fluorescent (RFP) protein with the modifications previously described (57). Tachyzoites expressing RFP were maintained in human fibroblasts (hTert cells) as described. For drug testing hTert cells were cultured in 96-well plates 24 h before infection, and $6x10^4$ cells were seeded in each well. On the day of the experiment freshly lysed parasites were purified by passing through a 27-gauge needle, followed by filtration through a 3-µm-pore-size membrane. Each well was seeded with 10^4 tachyzoites, and fluorescence values were followed for 5 days. The EC_{50} was calculated on day 5. Plates were read with covered lids, and both excitation (544 nm) and emission (590 nm) were read from the bottom. A Synergy H1 hybrid plate reader from BioTek was used to read fluorescence.

Statistical analysis.

All statistical analyses were performed using GraphPad Prism. Unless otherwise noted, all error bars are presented as the standard error of the mean (SEM) and from a minimum of three independent trials. Differences were considered significant if P values were < 0.05. ANOVA was used to compare larger than two sets of data. Comparison between two sets were done using T-test.

Data Availability

All the data is available in the main text or the supporting information.

Supporting Information

This article contains supporting information

Funding

This work was supported by the U.S. National Institutes of Health grants AI128356, AI154931 and AI174600 to SNJM. The computer work was partially supported by a Google research grant

to use on their Computer Platform. We acknowledge partial support from the NSF Advances in Biological Informatics (ABI) CAREER ABI-Innovation under award number 1845915 to SQ. KMN and MSF were partially supported through fellowships directly funded by a T32 training grant, T32 AI060546 or through fellowships awarded by the Office of Research to support the T32 training goals.

Acknowledgments

The authors thank Dr. Muthugapatti Kandasamy and the Biomedical Microscopy Core of the University of Georgia for the use of the microscopes. We thank Sebastian Lourido for the PKG M and T mutants used in Figure 4. We also thank Dominique Soldati for the gift of the *iΔPIPLC* mutants. Stephen A. Vella prepared the videos used for the analysis presented in Fig. 7C, D and E Omar Salas provided technical support and helped with the determination of the EC_{50}s.

FIGURES LEGENDS

Figure 1. Calcium entry through the plasma membrane of extracellular *T. gondii* tachyzoites. **(A)** Fura 2 loaded *T. gondii* tachyzoites at a concentration of $2x10^7$/ml are suspended in a buffer containing 100 μM EGTA (EGTA buffer). The resting Ca^{2+} represents the normal cytosolic concentration of Ca^{2+} $[Ca^{2+}]_{cyt}$. Addition of extracellular 1.8 mM Ca^{2+} stimulates Ca^{2+} entry as observed in the increase in cytosolic Ca^{2+} (basal Ca^{2+} entry). This increase is followed by a recovery. (**B**) Addition of extracellular Ca^{2+} (1.8 mM Ca^{2+}) to parasites suspended in EGTA buffer (*light blue trace*) or high Ca^{2+} buffer (1.8 mM Ca^{2+}, *gray trace*). T-Test: ** $p = 0.0018$. (**C**) 1.8 mM Ca^{2+} was added at various times after adding 100 μM EGTA: 200, 300, 400, 500 sec. Individual dots in the bar graphs represent biological replicates. Data was analyzed using One-Way ANOVA ** $p = 0.0082$, *** $p = 0.0005$, **** $p = 0.0001$. (**D**) The SERCA Ca^{2+}-ATPase inhibitor, thapsigargin (TG, 1 μM) was added at 100 sec followed by addition of 1.8 mM Ca^{2+} at 400 sec. Enhanced Ca^{2+} entry is highlighted. (**E**) TG was added in EGTA buffer (*blue trace*) or in high Ca^{2+} buffer (*gray trace*). The bar graph shows the rate of $[Ca^{2+}]_{cyt}$ increase. T-Test, * $p = 0.0133$. (**F**) Tachyzoites were in suspension in a buffer with 1.8 mM Ca^{2+}. 1.8 mM BAPTA (free acid) was added at 100 sec to the experiment represented by the dark pink trace. TG at 1 μM was added to both experiments. Individual dots represent the rate of Ca^{2+} increase for three biological replicates. Data was analyzed using Student's t -Test * $p = 0.0188$. (**G**) Parasites in suspension in a buffer without EGTA so the concentration of Ca^{2+} would be the contaminating one, ~10 μM. 100 μM EGTA was added at 100 sec and 1.8 mM BAPTA, free acid, right after adding 1.8 mM Ca^{2+}. The bar graph shows the slope values after adding BAPTA from three independent experiments. T-test: * $p = 0.0271$. (**H**) Parasites in suspension in EGTA buffer and TG was added at 100 sec. At 400 seconds 1.8 mM Ca^{2+} was added to both experiments and 1.8 mM BAPTA immediately after Ca^{2+} for the experiment represented by the pink trace. T-test *** $p = 0.003$. (**I**) 1.8 mM Ca^{2+} was added to parasites pre-incubated with the PMCA inhibitor Vanadate (*beige trace*) compared to the same experiment without Vanadate (*blue trace*). Parasites were suspended in EGTA buffer. T-test * $p = 0.0271$. All statistical analysis was done with data from three independent biological experiments.

Figure 2. Two types of Ca^{2+} channels are active at the PM in *T. gondii* tachyzoites. **(A)** Cytosolic concentration of Ca^{2+} obtained after adding the indicated extracellular Ca^{2+}. Values were taken from similar graphs as the one presented in S2A. $\Delta[Ca^{2+}]_i$ for the quantifications was calculated as $\Delta[Ca^{2+}]$ between the peak and basal Ca^{2+}**. (B)** 250 μM Ca^{2+} (*gray trace*) was added to a suspension of Fura 2 loaded tachyzoites in EGTA buffer compared with an identical experiment with parasites pre-incubated with 10 μM nifedipine (*red trace*). (**C**) Quantification of $\Delta[Ca^{2+}]_i$ in control and nifedipine treated parasites at various extracellular Ca^{2+} concentrations. Each dot represents an independent biological replicate. Data was analyzed using 2-way ANOVA, ** $p = 0.0047$, *** $p = 0.0001$, **** $p < 0.0001$. (**D**) Ca^{2+} entry stimulated with 250 μM extracellular Ca^{2+} (*gray trace*) compared with an identical experiment of cells pre-incubated with 1 μM ACA (*blue trace*). (**E**)

Quantification of $\Delta[Ca^{2+}]_i$ in control and ACA treated parasites after adding different concentrations of extracellular Ca^{2+}. Each dot represents an independent biological replicate. Data was analyzed using 2-way ANOVA analysis ns $p > 0.1$, ***$p = 0.0001$ and ****$p < 0.0001$. (**F**) Fura 2 loaded *T. gondii* tachyzoites in suspension. 1.8 mM Ca^{2+} was added were indicated. 10 µM Nifedipine or/and 1 µM ACA, were added at 50 sec or/and 150 sec, respectively. Each dot represents an independent biological replicate. Data was analyzed using One-way ANOVA analysis ** $p = 0.0012$, ** $p = 0.0083$ and * $p = 0.028$. (**G)** and (**H**) Parasites in suspension in EGTA buffer and pre-loaded with BAPTA-AM (iBAPTA). 1.8 mM extracellular Ca^{2+} was added at 400 seconds. The red trace in G represent an experiment with parasites pre-incubated with Nifedipine. The blue trace in H represent an experiment with parasites pre-incubated with anthranilic acid (ACA). **(I)** Quantification and statistical analysis of the $\Delta[Ca^{2+}]_i$ after adding extracellular Ca^{2+}. Individual dots represent biological replicates. Data was analyzed using One-way ANOVA analysis *** $p = 0.0006$, **** $p < 0.0001$. **(J)** Quantification and statistical analysis of $\Delta[Ca^{2+}]_i$ after adding extracellular Ca^{2+}, in the presence of inhibitors after chelating cytosolic Ca^{2+} with BAPTA. Each dot represents an independent biological replicate. Data was analyzed using One-way ANOVA analysis * $p = 0.04$, **** $p < 0.0001$. N, Nifedipine; A, ACA; C, control.

Figure 3. Calcium entry in *T. gondii* tachyzoites and the effect of Zaprinast. (**A**) Diagram illustrating Ca^{2+} entry and the potential participation of the cGMP signaling pathway stimulated by Zaprinast. (**B**) Extracellular tachyzoites in suspension loaded with Fura 2 treated with Zaprinast (Zap, 100 µM) at 100 sec and extracellular Ca^{2+} (1.8 mM) at 400 sec. Bar graph shows quantification of $\Delta[Ca^{2+}]_i$ after adding extracellular Ca^{2+} from more than 5 independent experiments. Each dot represents an independent biological replicate. Data was analyzed using Student's t-Test, ** $p = 0.0039$. (**C**) tachyzoites in buffer with 1.8 mM extracellular Ca^{2+}. Zaprinast (100 µM) was added at the indicated time by itself (*brown trace*) or preceded by the addition of 1.8 mM BAPTA (*green trace*). Bar graph shows the rate of cytosolic Ca^{2+} increase in response to Zap. Individual dots represent biological replicates. Data was analyzed using Student's t-Test * $p = 0.0354$. (**D**) Tachyzoites in EGTA buffer were first treated with 100 µM Zaprinast (100 sec) followed by the addition of 1.8 mM Ca^{2+} at 400 sec (*control, purple trace*). An identical experiment was done with parasites pre-incubated with 10 µM Nifedipine (*orange trace*). Bar graph shows quantification of $\Delta[Ca^{2+}]_i$ after adding extracellular Ca^{2+}. Each dot represents an independent biological replicate. Data was analyzed using Student's t-Test *** $p = 0.0003$. (**E)** Similar experiment to the one in D but replacing Nifedipine with 1 µM ACA. Bar graph shows quantification of $\Delta[Ca^{2+}]_i$ after adding extracellular Ca^{2+}. Each dot represents an independent biological replicate. Data was analyzed using Student's t-Test * $p = 0.02$. (**F**) Addition of 100 µM Zaprinast to parasites in suspension in a buffer containing 1.8 mM extracellular Ca^{2+} (*purple trace*) and the same experiment with parasites pre-incubated with Nifedipine (10 µM) (*orange trace*). Bar graph shows quantification of $\Delta[Ca^{2+}]_i$ after adding Zaprinast. Individual dots represent biological replicates. Data was analyzed using Student's t-Test ns $p = 0.8$. (**G**) Similar experiment

to the one in F but with 1 μM ACA. Each dot represents an independent biological replicate. Data was analyzed using Student's t-Test *p = 0.012.

Figure 4. Ca^{2+} entry and cyclicGMP (cGMP). **(A)** Fura 2-loaded extracellular tachyzoites in suspension were used. 200 μM cGMP was added to the suspension in EGTA buffer at 100 sec (*green and gray traces*). Extracellular Ca^{2+} (1.8 mM) was added at 400 sec. The gray trace shows a similar experiment with parasites pre-incubated with compound 1 (1 μM). The blue trace represents tachyzoites to which extracellular Ca^{2+} was added at 400 sec without extra additions (basal Ca^{2+} entry). (**B**) Compound 1 (Cpd1) (1 μM) was added (*maroon trace*) at 100 sec and extracellular Ca^{2+} (1.8 mM) was added at 400 sec. **(C)** Quantification and statistical analyses of the change in $[Ca^{2+}]_i$ measured after addition of extracellular Ca^{2+} without additions (*blue bar*) or after adding 200 μM cGMP (*green bar*), or 1 μM Cpd1 (*maroon bar*) or both (*dark gray bar*). Bar graphs represent the statistical analysis from three independent biological replicates using One-way ANOVA analysis *** p = 0.001, * p = 0.0343. Individual dots represent biological replicates. (**D**) and (**E**) Extracellular tachyzoites of the PKG-T mutant (see experimental details) loaded with Fura 2. 1 μM Cpd1 was added at 50 sec (*maroon trace*), 1.8 mM Ca^{2+} at 400 sec and 200 μM cGMP at 250 sec (*green trace in E*). Bar graphs show the quantification and statistical analysis of $\Delta[Ca^{2+}]_i$ after adding extracellular Ca^{2+}. Individual dots represent biological replicates. Data was analyzed with Student's t-Test * $p < 0.05$. (**F**) and (**G**) Similar experiments and conditions to the ones used in D and E but using the PKG-M strain, which expressed PKG ($T^{761}M$) resistant to Cpd 1. Individual dots represent biological replicates. Data was analyzed using Student's t-Test ns $p > 0.05$.

Figure 5. The role of PI-PLC in Ca^{2+} entry. **(A)** Diagram illustrating a model of the role of cGMP, PKG and PI-PLC in Ca^{2+} entry. (**B**) Fura-2 loaded tachyzoites in EGTA buffer (100 μM EGTA). 1 μM U73122 (*brown trace*) or U73343 (*green trace*) were added at 50 sec. 200 μM cGMP and 1.8 mM extracellular Ca^{2+} were added where indicated. Bar graphs show the statistical analysis from three independent biological replicates using One-way ANOVA, ns p = 0.08, ** $p < 0.002$. Individual dots represent biological replicates. (**C**) the experimental set-up was similar to the one presented in B but parasites were pre-incubated with 10 μM Nifedipine (*orange trace*) and U73122 was added at 50 sec. Statistical analysis of three independent experiments using t-Test ** p = 0.003. For experiments shown in **D-K**, extracellular tachyzoites of the *iΔPIPLC* mutant (± ATc for 48) were Fura-2-loaded. Tachyzoites were in suspension in EGTA buffer and 1.8 mM Ca^{2+} was added at 400 sec. Pink traces represents the results with the mutant pre-incubated with ATc and green traces represent the same mutant without ATc. **(D)** the basal Ca^{2+} entry was measured by adding 1.8 mM Ca^{2+} at 400 sec. **(E)** At 100 sec, 1 μM Thapsigargin (TG) was added and 1.8 mM Ca^{2+} at 400 sec. **(F)** quantification of the $\Delta[Ca^{2+}]_i$ from parts D and E. ANOVA analysis ** p = 0.001, ** p = 0.005 and ns p > 0.05. **(G)** Similar experiment to the one in **E** but with 100 μM Zaprinast added at 100 sec. Data was analyzed using One-way ANOVA, *** p= 0.0004, ** p= 0.005 and ns $p > 0.05$. Each dot represents an independent biological replicate**. (H)** Similar experiment to the one in G but 1 μM U73122 was added at 100 sec, followed by 1.8 mM Ca^{2+} at

400 sec. Individual dots represent biological replicates. One-way ANOVA, ** $p = 0.003$ and ns $p > 0.05$. **(I)** Identical set-up to H but the inactive analogue U73343 was added at 100 sec. Data from three biological experiments was analyzed using One-way ANOVA ns $p > 0.05$. For G, H, and I, the one-way ANOVA analysis includes the Ca^{2+} basal control data from F. (**J**) Similar experiment to the one shown in D with tachyzoites (+ATc) pre-incubated with Nifedipine, 10 μM (*gray trace*). Individual dots represent biological replicates. Data was analyzed using Student's t-Test * $p = 0.014$. (**K**) Similar experimental set-up with 200 μM cGMP added at 100 sec and 1.8 mM Ca^{2+} at 400 sec. The dotted pink trace represents the result with the *iΔPIPLC* mutant (+ATc for 48 h) pre-incubated with 10 μM Nif. Individual dots represent biological replicates. Data was analyzed using One-way ANOVA, **$p = 0.009$, **$p = 0.002$, *$p = 0.01$ and ns $p > 0.05$. Bar graphs for B-K shows the statistical analysis of a minimum of three independent experiments for which the $\Delta[Ca^{2+}]_i$ was measured.

Figure 6. Extracellular Calcium and *T. gondii* growth and invasion. **(A)** Plaque assays of *T. gondii* RH tachyzoites cultured in regular growth media without Ca^{2+} and supplemented with Ca^{2+} 1.8 mM, 0.5 mM or 0.25 mM Ca^{2+}. Confluent fibroblast cells were infected with 200 tachyzoites for 8 days. The bar graph shows the quantification of the plaque areas from a minimum of 4 independent experiments. Individual dots represent biological replicates. Data was analyzed using One-way ANOVA, ****$p < 0.0001$. (**B**) Plaque assays of *T. gondii* RH tachyzoites grown in regular media in the presence of the indicated inhibitors. Cilnedipine, 40 μM; Compound 1 (Cpd1), 1 μM; Anthranilic acid (ACA), 1 μM. The bar graph shows the quantification of the plaque areas from a minimum of 4 independent experiments. Statistical analysis was done using One-way ANOVA, ****$p < 0.0001$. Individual dots represent biological replicates. **(C)** Invasion and attachment experiments using the red/green assay of tachyzoites. Confluent fibroblast monolayers were infected with 2×10^7 tachyzoites. Inhibitors were added 5 min prior to the invasion step. Parasites were stained with RabbitαSAG1 at 1:1,000 dilution and MouseαSAG1 at 1:200 dilution. Secondary antibodies were goat-αRabbit and Alexa Flour 546 and Alexa Flour 488 goat-αMouse, both at 1:1,000 dilution. C, control; Nif, nifedipine, 10 μM; ACA, anthranilic acid, 1 μM; Zap, zaprinast, 100 μM; U22, U73122 1 μM; U33, U73233, 1 μM. 100% is the sum of parasites that have either attached or invaded the host cell in 10 fields of view. Individual dots represent biological replicates. Data was analyzed using One-way ANOVA * $p < 0.05$, ** $p < 0.001$ and **** $p < 0.0001$.

Figure 7. Calcium entry and egress. **(A)** control experiment in EGTA buffer (100 μM EGTA). 0.01% saponin was added at 50 sec. Fluorescence of single parasites were analyzed with FIJI. F/F_0 represents the normalized fluorescence of single parasites to the resting fluorescence prior to adding saponin. The bar graph shows the statistical analysis of the time to egress (of the leading parasite) from a minimum of three independent experiments. T-Test analysis, ** $p = 0.004$. Scale bars = 5 μm. **(B)** Similar experimental set-up to the one in **A** but the buffer contains 1.8 mM Ca^{2+}. Bar graph shows quantification of time of egress for the leading parasite of the vacuole. T-Test

analysis ns $p = 0.006$. Scale bars = 5 μm. **(C)** GCaMP6f expressing parasites immobilized in 10% FBS were preincubated with ACA, cilnidipine or nifedipine. After 1 minute of video recording 1.8 mM Ca^{2+} was added. Violin plot of relative distance shows parasites distribution before and after Ca^{2+} addition. T-test **** $p < 0.0004$. **(D) and (E)** Relative distance travel by the tachyzoites after 100 μM Zaprinast addition in low (D) and high (E) Ca^{2+} buffer. Plot shows data from three independent biological experiments T-test ****$p < 0.0001$, **$p < 0.005$ and T-test **$p < 0.005$, *$p < 0.05$ respectively.

Figure 8. Proposed model for the regulation of PM Ca^{2+} entry of tachyzoites of *Toxoplasma gondii*. cGMP activates PKG which may activate PI-PLC through phosphorylation. Ca^{2+} is also essential for PIPLC activity which results in the hydrolysis of phosphatidylinositol 4,5-bisphosphate to form inositol trisphosphate or IP_3 which will open an unknown Ca^{2+} release channel at the ER releasing Ca^{2+} into the cytosol. This Ca^{2+} increase stimulates Ca^{2+} entry through a TRP-like channel. The inhibition by Nifedipine and ACA of different channels is shown.

References

1. Weiss, L. M., and Dubey, J. P. (2009) Toxoplasmosis: A history of clinical observations. Int J Parasitol **39**, 895-901 10.1016/j.ijpara.2009.02.004
2. Black, M. W., and Boothroyd, J. C. (2000) Lytic cycle of *Toxoplasma gondii*. Microbiol Mol Biol Rev **64**, 607-623, http://www.ncbi.nlm.nih.gov/pubmed/10974128
3. Blader, I. J., Coleman, B. I., Chen, C. T., and Gubbels, M. J. (2015) Lytic Cycle of *Toxoplasma gondii*: 15 Years Later. Annu Rev Microbiol **69**, 463-485 10.1146/annurev-micro-091014-104100
4. Lourido, S., and Moreno, S. N. (2015) The calcium signaling toolkit of the Apicomplexan parasites *Toxoplasma gondii* and *Plasmodium* spp. Cell Calcium **57**, 186-193 10.1016/j.ceca.2014.12.010
5. Hortua Triana, M. A., Marquez-Nogueras, K. M., Vella, S. A., and Moreno, S. N. J. (2018) Calcium signaling and the lytic cycle of the Apicomplexan parasite *Toxoplasma gondii*. Biochim Biophys Acta Mol Cell Res **1865**, 1846-1856 10.1016/j.bbamcr.2018.08.004
6. Clapham, D. E. (2007) Calcium signaling. Cell **131**, 1047-1058 10.1016/j.cell.2007.11.028
7. Bootman, M. D., and Bultynck, G. (2020) Fundamentals of Cellular Calcium Signaling: A Primer. Cold Spring Harb Perspect Biol **12**, 10.1101/cshperspect.a038802
8. Lovett, J. L., and Sibley, L. D. (2003) Intracellular calcium stores in *Toxoplasma gondii* govern invasion of host cells. J Cell Sci **116**, 3009-3016 10.1242/jcs.00596
9. Borges-Pereira, L., Budu, A., McKnight, C. A., Moore, C. A., Vella, S. A., Hortua Triana, M. A. *et al.* (2015) Calcium Signaling throughout the *Toxoplasma gondii* Lytic Cycle: A STUDY USING GENETICALLY ENCODED CALCIUM INDICATORS. J Biol Chem **290**, 26914-26926 10.1074/jbc.M115.652511
10. Pace, D. A., McKnight, C. A., Liu, J., Jimenez, V., and Moreno, S. N. (2014) Calcium entry in *Toxoplasma gondii* and its enhancing effect of invasion-linked traits. J Biol Chem **289**, 19637-19647 10.1074/jbc.M114.565390
11. Vella, S. A., Moore, C. A., Li, Z. H., Hortua Triana, M. A., Potapenko, E., and Moreno, S. N. J. (2021) The role of potassium and host calcium signaling in *Toxoplasma gondii* egress. Cell Calcium **94**, 102337 10.1016/j.ceca.2020.102337
12. Marquez-Nogueras, K. M., Hortua Triana, M. A., Chasen, N. M., Kuo, I. Y., and Moreno, S. N. (2021) Calcium signaling through a transient receptor channel is important for *Toxoplasma gondii* growth. Elife **10**, 10.7554/eLife.63417
13. Bird, G. S., DeHaven, W. I., Smyth, J. T., and Putney, J. W., Jr. (2008) Methods for studying store-operated calcium entry. Methods **46**, 204-212 10.1016/j.ymeth.2008.09.009
14. Putney, J. W. (2017) Store-Operated Calcium Entry: An Historical Overview. Adv Exp Med Biol **981**, 205-214 10.1007/978-3-319-55858-5_9
15. Prole, D. L., and Taylor, C. W. (2011) Identification of intracellular and plasma membrane calcium channel homologues in pathogenic parasites. PLoS One **6**, e26218 10.1371/journal.pone.0026218
16. Brown, K. M., and Sibley, L. D. (2018) Essential cGMP Signaling in Toxoplasma Is Initiated by a Hybrid P-Type ATPase-Guanylate Cyclase. Cell Host Microbe **24**, 804-816 e806 10.1016/j.chom.2018.10.015

17. Bisio, H., and Soldati-Favre, D. (2019) Signaling Cascades Governing Entry into and Exit from Host Cells by *Toxoplasma gondii*. Annu Rev Microbiol **73**, 579-599 10.1146/annurev-micro-020518-120235
18. Petri, E. T., Celic, A., Kennedy, S. D., Ehrlich, B. E., Boggon, T. J., and Hodsdon, M. E. (2010) Structure of the EF-hand domain of polycystin-2 suggests a mechanism for Ca2+-dependent regulation of polycystin-2 channel activity. Proc Natl Acad Sci U S A **107**, 9176-9181 10.1073/pnas.0912295107
19. Ryu, S. H., Suh, P. G., Cho, K. S., Lee, K. Y., and Rhee, S. G. (1987) Bovine brain cytosol contains three immunologically distinct forms of inositolphospholipid-specific phospholipase C. Proc Natl Acad Sci U S A **84**, 6649-6653 10.1073/pnas.84.19.6649
20. Horowitz, L. F., Hirdes, W., Suh, B. C., Hilgemann, D. W., Mackie, K., and Hille, B. (2005) Phospholipase C in living cells: activation, inhibition, Ca2+ requirement, and regulation of M current. J Gen Physiol **126**, 243-262 10.1085/jgp.200509309
21. Lam, A. K., and Galione, A. (2013) The endoplasmic reticulum and junctional membrane communication during calcium signaling. Biochim Biophys Acta **1833**, 2542-2559 10.1016/j.bbamcr.2013.06.004
22. Moreno, S. N., and Zhong, L. (1996) Acidocalcisomes in *Toxoplasma gondii* tachyzoites. Biochem J **313 (Pt 2)**, 655-659, http://www.ncbi.nlm.nih.gov/pubmed/8573106
23. Nagamune, K., Beatty, W. L., and Sibley, L. D. (2007) Artemisinin induces calcium-dependent protein secretion in the protozoan parasite *Toxoplasma gondii*. Eukaryot Cell **6**, 2147-2156 10.1128/EC.00262-07
24. Vercesi, A. E., Moreno, S. N., Bernardes, C. F., Meinicke, A. R., Fernandes, E. C., and Docampo, R. (1993) Thapsigargin causes Ca2+ release and collapse of the membrane potential of *Trypanosoma brucei* mitochondria in situ and of isolated rat liver mitochondria. J Biol Chem **268**, 8564-8568, https://www.ncbi.nlm.nih.gov/pubmed/8473301
25. Brini, M. (2009) Plasma membrane Ca(2+)-ATPase: from a housekeeping function to a versatile signaling role. Pflugers Arch **457**, 657-664 10.1007/s00424-008-0505-6
26. Brini, M., Bano, D., Manni, S., Rizzuto, R., and Carafoli, E. (2000) Effects of PMCA and SERCA pump overexpression on the kinetics of cell Ca(2+) signalling. EMBO J **19**, 4926-4935 10.1093/emboj/19.18.4926
27. Luo, S., Vieira, M., Graves, J., Zhong, L., and Moreno, S. N. (2001) A plasma membrane-type Ca(2+)-ATPase co-localizes with a vacuolar H(+)-pyrophosphatase to acidocalcisomes of *Toxoplasma gondii*. EMBO J **20**, 55-64 10.1093/emboj/20.1.55
28. Luo, S., Ruiz, F. A., andMoreno, S. N. (2005) The acidocalcisome Ca2+-ATPase (TgA1) of *Toxoplasma gondii* is required for polyphosphate storage, intracellular calcium homeostasis and virulence. Mol Microbiol **55**, 1034-1045 10.1111/j.1365-2958.2004.04464.x
29. Zamponi, G. W., Striessnig, J., Koschak, A., and Dolphin, A. C. (2015) The Physiology, Pathology, and Pharmacology of Voltage-Gated Calcium Channels and Their Future Therapeutic Potential. Pharmacol Rev **67**, 821-870 10.1124/pr.114.009654
30. Prasher, P., and Sharma, M. (2021) Medicinal chemistry of anthranilic acid derivatives: A mini review. Drug Dev Res **82**, 945-958 10.1002/ddr.21842

31. Sidik, S. M., Hortua Triana, M. A., Paul, A. S., El Bakkouri, M., Hackett, C. G., Tran, F. *et al.* (2016) Using a Genetically Encoded Sensor to Identify Inhibitors of *Toxoplasma gondii* Ca2+ Signaling. J Biol Chem **291**, 9566-9580 10.1074/jbc.M115.703546
32. Donald, R. G., Allocco, J., Singh, S. B., Nare, B., Salowe, S. P., Wiltsie, J. *et al.* (2002) *Toxoplasma gondii* cyclic GMP-dependent kinase: chemotherapeutic targeting of an essential parasite protein kinase. Eukaryot Cell **1**, 317-328, https://www.ncbi.nlm.nih.gov/pubmed/12455981
33. Brown, K. M., Tonkin, C. J., Billker, O., and Sibley, L. D. (2020) Calcium and cyclic nucleotide signaling networks in *Toxoplasma gondii*. In *Toxoplasma gondii*. The Model Apicomplexan-Perspectives and Methods, Third Ed. Kim LMWaK, ed. Academic Press, Chapter 13, 577-605
34. Bleasdale, J. E., Thakur, N. R., Gremban, R. S., Bundy, G. L., Fitzpatrick, F. A., Smith, R. J. *et al.* (1990) Selective inhibition of receptor-coupled phospholipase C-dependent processes in human platelets and polymorphonuclear neutrophils. J Pharmacol Exp Ther **255**, 756-768, https://www.ncbi.nlm.nih.gov/pubmed/2147038
35. Smith, R. J., Sam, L. M., Justen, J. M., Bundy, G. L., Bala, G. A., and Bleasdale, J. E. (1990) Receptor-coupled signal transduction in human polymorphonuclear neutrophils: effects of a novel inhibitor of phospholipase C-dependent processes on cell responsiveness. J Pharmacol Exp Ther **253**, 688-697, https://www.ncbi.nlm.nih.gov/pubmed/2338654
36. Bullen, H. E., Jia, Y., Yamaryo-Botte, Y., Bisio, H., Zhang, O., Jemelin, N. K. *et al.* (2016) Phosphatidic Acid-Mediated Signaling Regulates Microneme Secretion in Toxoplasma. Cell Host Microbe **19**, 349-360 10.1016/j.chom.2016.02.006
37. Fazli, M. S., Vella, S. A., Moreno, S. N. J., and Quinn, S. (2018) Unsupervised Discovery of Toxoplasma Gondii Motility Phenotypes. 2018 Ieee 15th International Symposium on Biomedical Imaging (Isbi 2018) 981-984, <Go to ISI>://WOS:000455045600224
38. Elaib, Z., Saller, F., and Bobe, R. (2016) The Calcium Entry-Calcium Refilling Coupling. Adv Exp Med Biol **898**, 333-352 10.1007/978-3-319-26974-0_14
39. Rizzuto, R., andPozzan, T. (2006) Microdomains of intracellular Ca2+: molecular determinants and functional consequences. Physiol Rev **86**, 369-408 10.1152/physrev.00004.2005
40. Brown, K. M., Long, S., and Sibley, L. D. (2017) Plasma Membrane Association by N-Acylation Governs PKG Function in *Toxoplasma gondii*. MBio **8**, 10.1128/mBio.00375-17
41. Donald, R. G., Zhong, T., Wiersma, H., Nare, B., Yao, D., Lee, A. *et al.* (2006) Anticoccidial kinase inhibitors: identification of protein kinase targets secondary to cGMP-dependent protein kinase. Mol Biochem Parasitol **149**, 86-98 10.1016/j.molbiopara.2006.05.003
42. Donald, R. G., and Liberator, P. A. (2002) Molecular characterization of a coccidian parasite cGMP dependent protein kinase. Mol Biochem Parasitol **120**, 165-175, https://www.ncbi.nlm.nih.gov/pubmed/11897122
43. Gurnett, A. M., Liberator, P. A., Dulski, P. M., Salowe, S. P., Donald, R. G., Anderson, J. W. *et al.* (2002) Purification and molecular characterization of cGMP-dependent

protein kinase from Apicomplexan parasites. A novel chemotherapeutic target. J Biol Chem **277**, 15913-15922 10.1074/jbc.M108393200
44. Wiersma, H. I., Galuska, S. E., Tomley, F. M., Sibley, L. D., Liberator, P. A., andDonald, R. G. (2004) A role for coccidian cGMP-dependent protein kinase in motility and invasion. Int J Parasitol **34**, 369-380 10.1016/j.ijpara.2003.11.019
45. Baker, D. A., andDeng, W. (2005) Cyclic GMP-dependent protein kinases in protozoa. Front Biosci **10**, 1229-1238 10.2741/1615
46. Yang, L., Uboldi, A. D., Seizova, S., Wilde, M. L., Coffey, M. J., Katris, N. J. *et al.* (2019) An apically located hybrid guanylate cyclase-ATPase is critical for the initiation of Ca(2+) signaling and motility in *Toxoplasma gondii*. J Biol Chem **294**, 8959-8972 10.1074/jbc.RA118.005491
47. Fang, J., Marchesini, N., and Moreno, S. N. (2006) A *Toxoplasma gondii* phosphoinositide phospholipase C (TgPI-PLC) with high affinity for phosphatidylinositol. Biochem J **394**, 417-425 10.1042/BJ20051393
48. Alam, M. M., Solyakov, L., Bottrill, A. R., Flueck, C., Siddiqui, F. A., Singh, S. *et al.* (2015) Phosphoproteomics reveals malaria parasite Protein Kinase G as a signalling hub regulating egress and invasion. Nat Commun **6**, 7285 10.1038/ncomms8285
49. Herneisen, A. L., Li, Z. H., Chan, A. W., Moreno, S. N. J., and Lourido, S. (2022) Temporal and thermal profiling of the *Toxoplasma* proteome implicates parasite Protein Phosphatase 1 in the regulation of Ca(2+)-responsive pathways. Elife **11**, 10.7554/eLife.80336
50. Brochet, M., Collins, M. O., Smith, T. K., Thompson, E., Sebastian, S., Volkmann, K. *et al.* (2014) Phosphoinositide metabolism links cGMP-dependent protein kinase G to essential Ca(2)(+) signals at key decision points in the life cycle of malaria parasites. PLoS Biol **12**, e1001806 10.1371/journal.pbio.1001806
51. Farwell, D. G., Shera, K. A., Koop, J. I., Bonnet, G. A., Matthews, C. P., Reuther, G. W. *et al.* (2000) Genetic and epigenetic changes in human epithelial cells immortalized by telomerase. Am J Pathol **156**, 1537-1547 10.1016/S0002-9440(10)65025-0
52. Stasic, A. J., Dykes, E. J., Cordeiro, C. D., Vella, S. A., Fazli, M. S., Quinn, S. *et al.* (2021) Ca(2+) entry at the plasma membrane and uptake by acidic stores is regulated by the activity of the V-H(+) -ATPase in Toxoplasma gondii. Mol Microbiol **115**, 1054-1068 10.1111/mmi.14722
53. Grynkiewicz, G., Poenie, M., and Tsien, R. Y. (1985) A new generation of Ca2+ indicators with greatly improved fluorescence properties. J Biol Chem **260**, 3440-3450, https://www.ncbi.nlm.nih.gov/pubmed/3838314
54. Liu, J., Pace, D., Dou, Z., King, T. P., Guidot, D., Li, Z. H. *et al.* (2014) A vacuolar-H(+) -pyrophosphatase (TgVP1) is required for microneme secretion, host cell invasion, and extracellular survival of *Toxoplasma gondii*. Mol Microbiol **93**, 698-712 10.1111/mmi.12685
55. Schindelin, J., Arganda-Carreras, I., Frise, E., Kaynig, V., Longair, M., Pietzsch, T. *et al.* (2012) Fiji: an open-source platform for biological-image analysis. Nat Methods **9**, 676-682 10.1038/nmeth.2019
56. Kafsack, B. F., Beckers, C., and Carruthers, V. B. (2004) Synchronous invasion of host cells by Toxoplasma gondii. Mol Biochem Parasitol **136**, 309-311, https://www.ncbi.nlm.nih.gov/pubmed/15478810

57. Szajnman, S. H., Galaka, T., Li, Z. H., Li, C., Howell, N. M., Chao, M. N. *et al.* (2017) In Vitro and In Vivo Activities of Sulfur-Containing Linear Bisphosphonates against Apicomplexan Parasites. Antimicrob Agents Chemother **61**, 10.1128/AAC.01590-16

TABLES:

Table 1: Percentage of inhibition of Ca^{2+} entry.

COMPOUNDS	% Inhibition*
40 μM Cilnidipine	78.8 ± 4.6
10 μM Nifedipine	84.7 ± 5.7
100 μM Verapamil	42.7 ± 2.3
1 μM ACA	50.3 ± 10.7

*Control (0%) was established as Ca^{2+} entry as shown in Fig 1A without inhibitor.
± Standard error was calculated with four independent experiments.

Table 2: Nifedipine inhibition of Ca^{2+} entry at various extracellular [Ca^{2+}]

$[Ca^{2+}]_E$ (mM)	% Inhibition by NIF*
0.1	98.59 ± 0.44
0.25	96.54 ± 0.83
0.5	97.24 ± 0.95
1	86.05 ± 4.59
1.8	64.84 ± 4.95

* NIF = Nifedipine

Table 3: Inhibition of growth by calcium related inhibitors and channels blockers (EC_{50}).

COMPOUNDS	EC_{50} (μM)*
Cilnidipine	3.5 ± 1.7
Nifedipine	N/A
Verapamil	30.7 ± 6.9
ACA	1.6 ± 0.3
Compound 1	0.11 ± 0.04
Zaprinast	200**
U73122	0.35 ± 0.1
U73343	2.4 ± 0.8

(N/A): Not possible to determine due to instability of the compound.
*: The EC_{50} was calculated from three independent growth experiments
**: Sidik et al, 2016

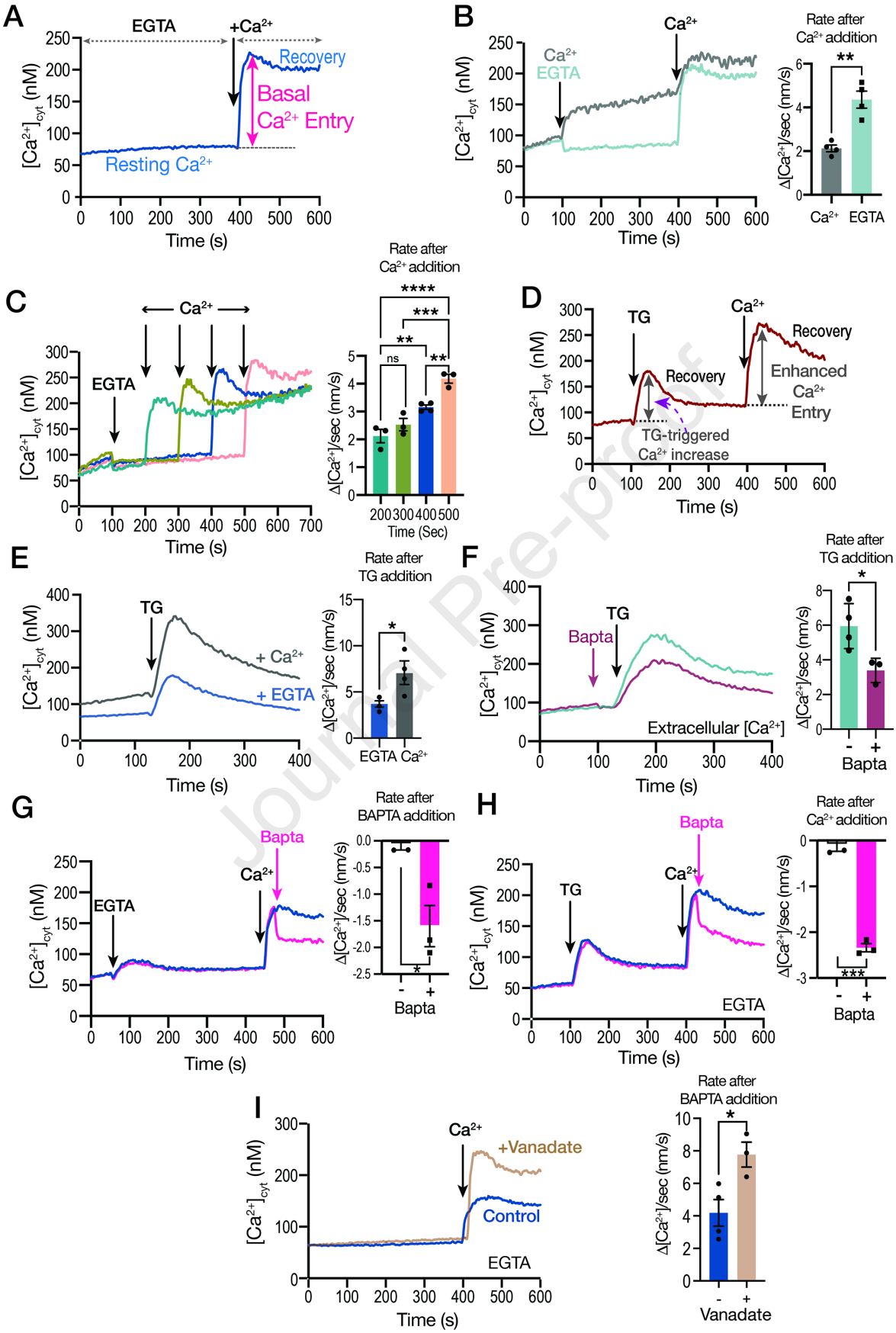

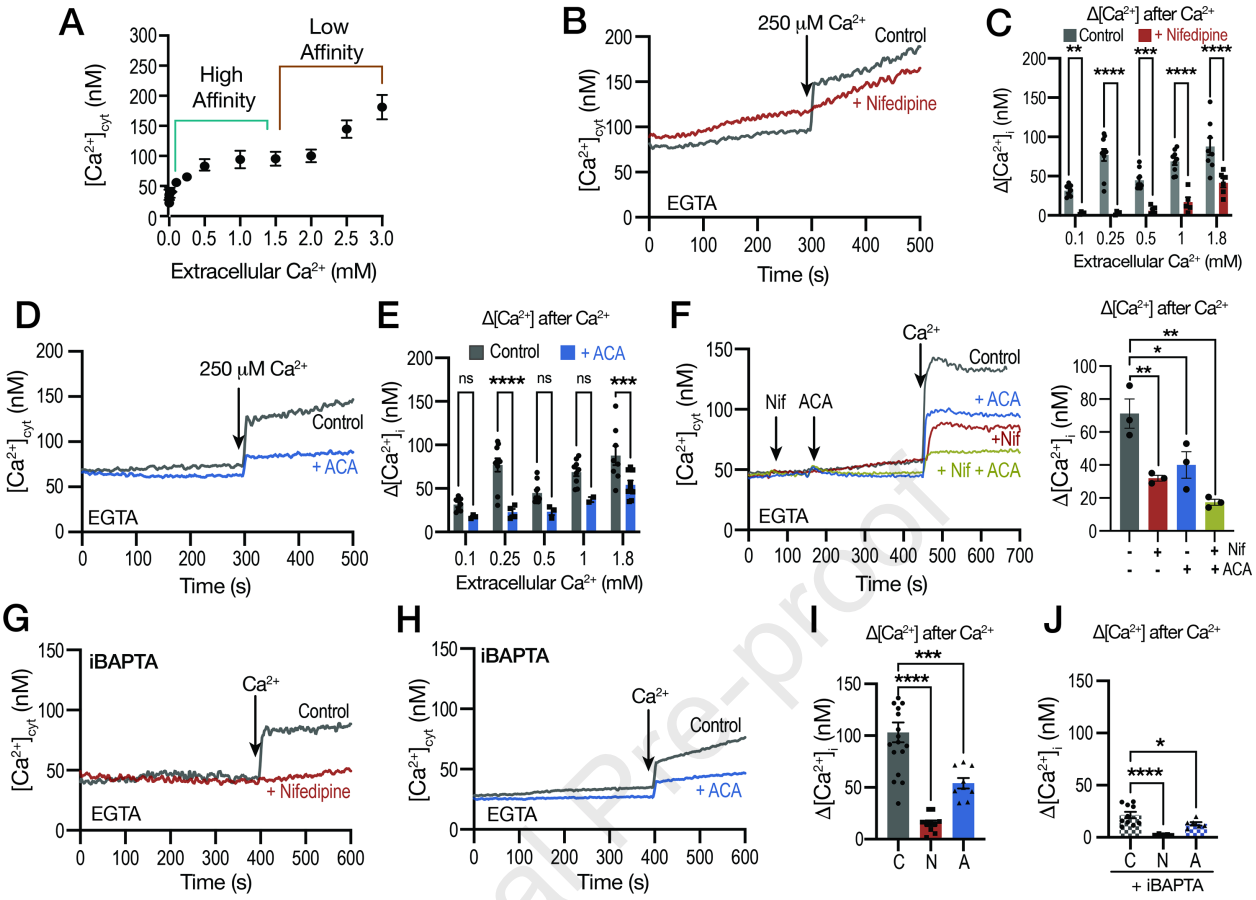

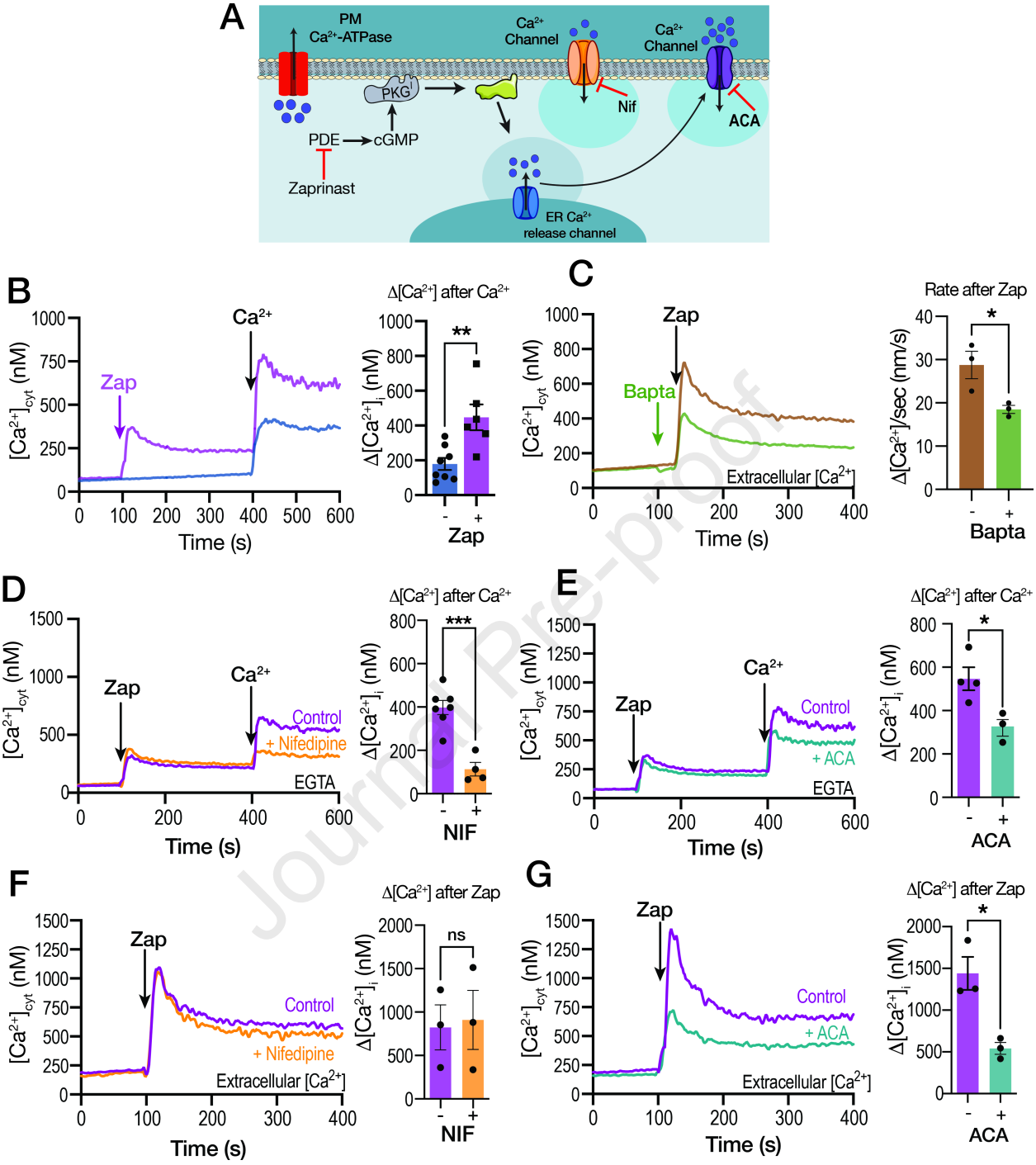

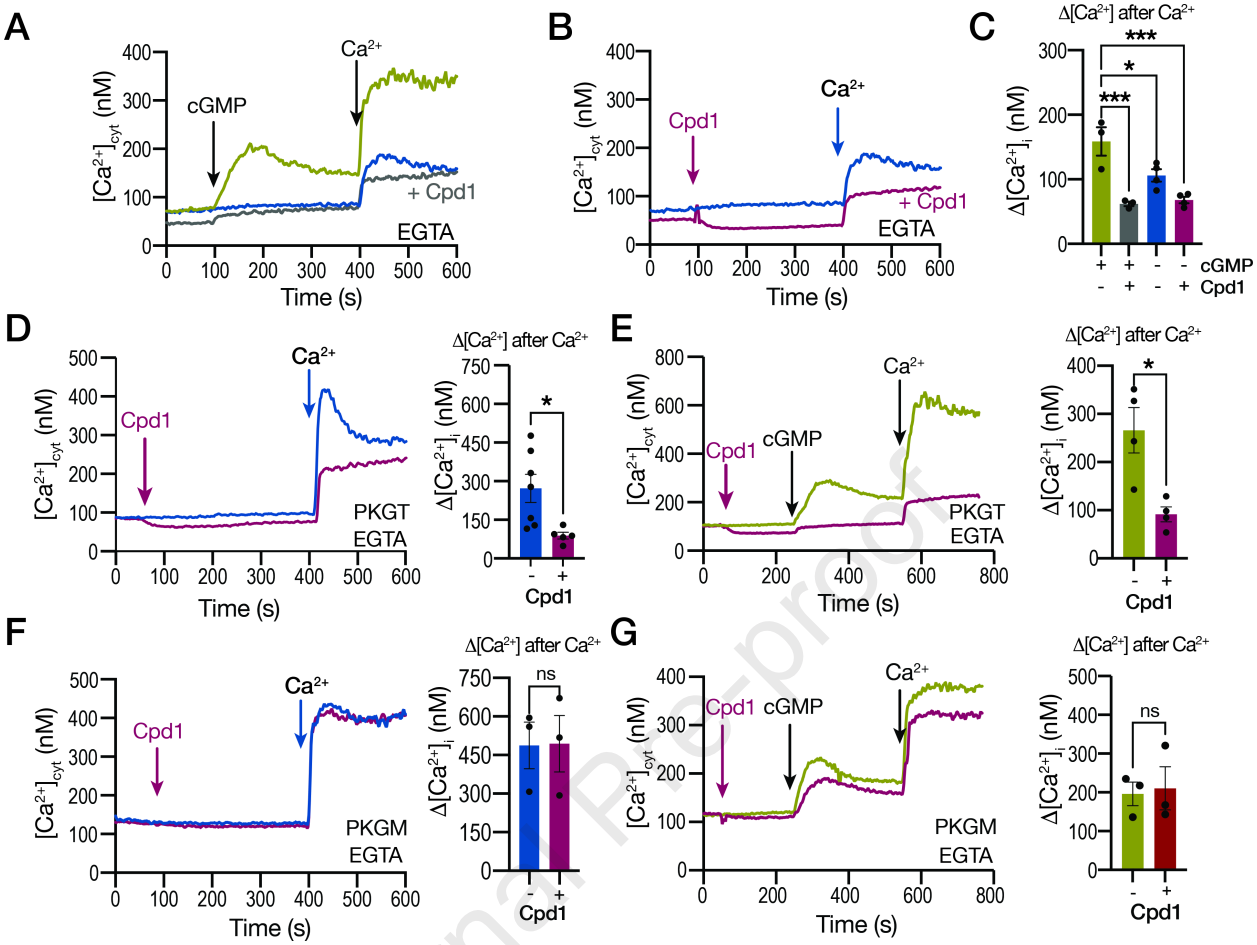

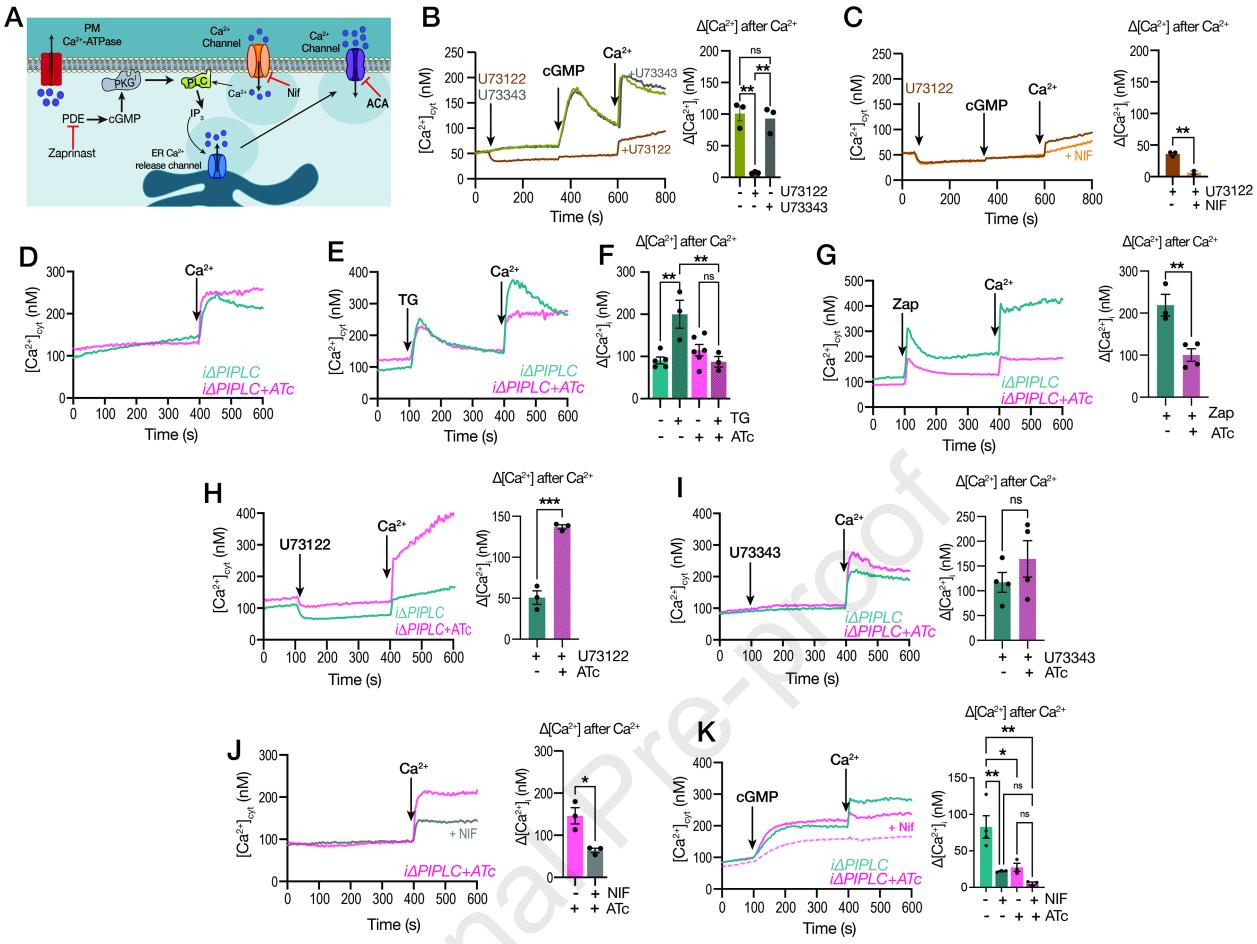

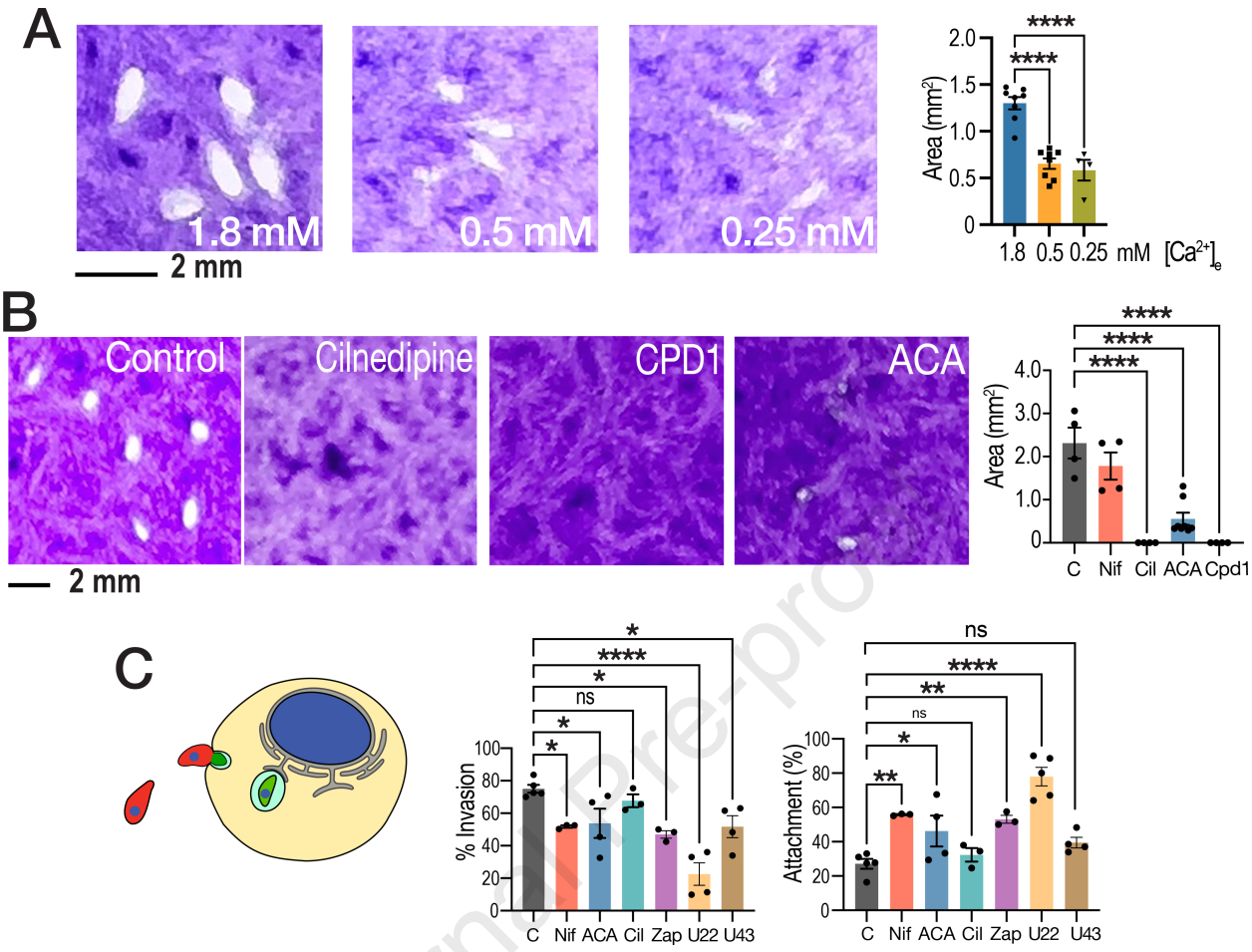

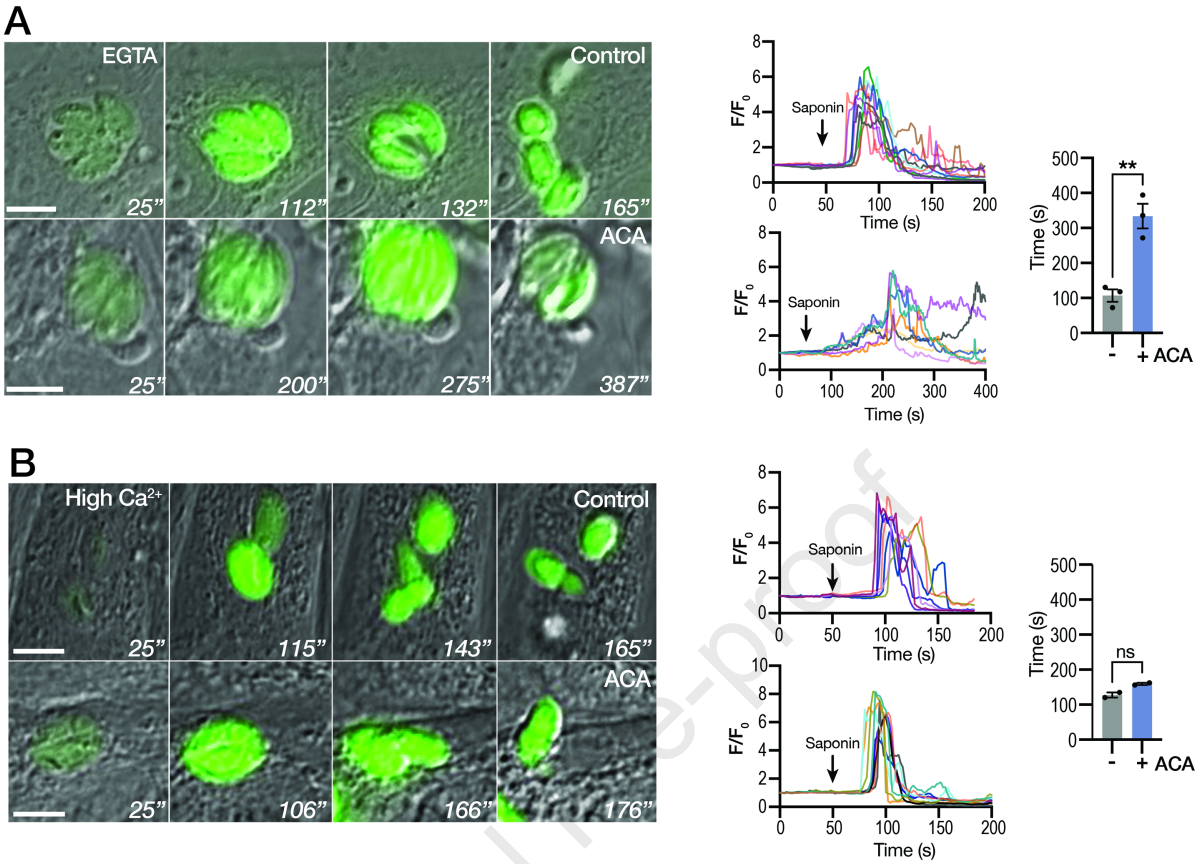

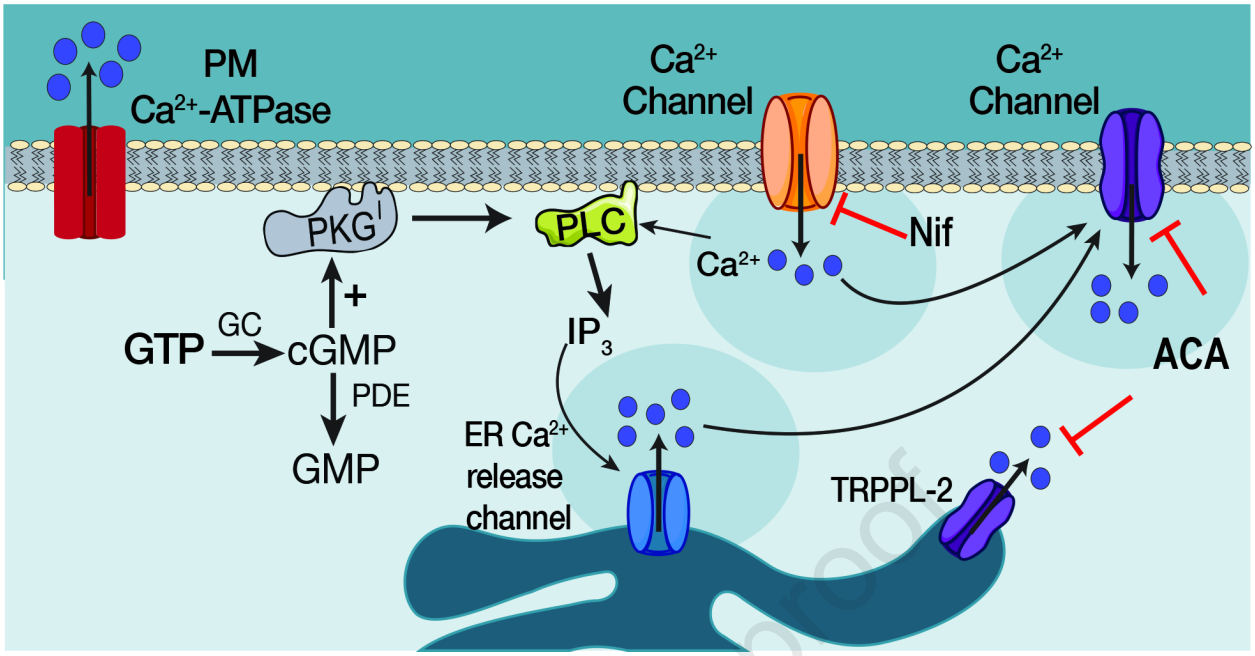

Author's contributions:

Myriam Andrea Hortua Triana: Conceptualization, methodology, investigation, original draft preparation. **Karla Marquez Nogueras**: made the growth assay experiments and the initial calcium experiments and analyzed the data. **Mojtaba Sedigh Fazli** and **Shannon Quinn**: developed a motility algorithm to follow motility and Calcium. **Silvia N J Moreno**: supervised the project, writing, reviewing and editing.

Declaration of interests

☒ The authors declare that they have no known competing financial interests or personal relationships that could have appeared to influence the work reported in this paper.